A PHENOMENOLOGICAL MODEL FOR THE MOMENTUMLESS TURBULENT WAKE IN A STRATIFIED MEDIUM

D. R. S. Ko

TRW Systems Group

Prepared for:

Office of Naval Research

April 1973

20086-6007-RU-00

WAKE MIXING STUDIES

15 August 1971 - 30 June 1973

Final Report

A PHENOMENOLOGICAL MODEL FOR THE MOMENTUMLESS TURBULENT WAKE IN A STRATIFIED MEDIUM

1973 April

Sponsored by

Advanced Research Projects Agency
ARPA Order No. 1910
Program Code No. 3E20

Monitored by

Office of Naval Research
Arlington, Virginia
Contract N00014-72-C-0074

The views and conclusions contained in this document are those of the author and should not be interpreted as necessarily representing the official policies, either expressed or implied, of the Advanced Research Projects Agency or the U. S. Government.

TRW
SYSTEMS GROUP
ONE SPACE PARK, REDONDO BEACH, CALIFORNIA 90278

20086-6007-RU-00

WAKE MIXING STUDIES

15 August 1971 - 30 June 1973

Final Report

A PHENOMENOLOGICAL MODEL FOR THE MOMENTUMLESS TURBULENT WAKE IN A STRATIFIED MEDIUM

1973 April

Sponsored by

Advanced Research Projects Agency
ARPA Order No. 1910
Program Code No. 3E20

Monitored by

Office of Naval Research
Arlington, Virginia
Contract N00014-72-C-0074

The views and conclusions contained in this document are those of the author and should not be interpreted as necessarily representing the official policies, either expressed or implied, of the Advanced Research Projects Agency or the U. S. Government.

TRW
SYSTEMS GROUP
ONE SPACE PARK, REDONDO BEACH, CALIFORNIA 90278

UNCLASSIFIED

Security Classification

DOCUMENT CONTROL DATA · R&D

(Security classification of title, body of abstract and indexing annotation must be entered when the overall report is classified)

1 ORIGINATING ACTIVITY (Corporate author)

TRW Systems Group

2a REPORT SECURITY CLASSIFICATION

Unclassified

2b GROUP

3 REPORT TITLE

A PHENOMENOLOGICAL MODEL FOR THE MOMENTUMLESS TURBULENT WAKE IN A STRATIFIED MEDIUM

4 DESCRIPTIVE NOTES (Type of report and inclusive dates)

Technical Final Report

5 AUTHOR(S) (Last name, first name, initial)

Ko, D. R. S., Flow Research, Inc. (TRW Subcontract No. 010CH3E)

6 REPORT DATE	7a TOTAL NO OF PAGES	7b NO OF REFS
1973 April	50	10

8a CONTRACT OR GRANT NO	9a ORIGINATOR'S REPORT NUMBER(S)
N00014-72-C-0074 b PROJECT NO ARPA Order No. 1910 Program Code No. 3E20	20086-6007-RU-00 9b OTHER REPORT NO(S) (Any other numbers that may be assigned this report)

10 AVAILABILITY/LIMITATION NOTICES

11 SUPPLEMENTARY NOTES	12 SPONSORING MILITARY ACTIVITY
	Office of Naval Research Arlington, Virginia

13 ABSTRACT

A simple phenomenological model, including non-uniform entrainment rate, is formulated by the growth and the collapse of a momentumless turbulent wake in a stratified medium. A series of parametric studies have been performed to study the effect of various operational conditions as well as the initial conditions on the wake flow field.

A solution was found to be sensitive to some initial conditions. The physical significance, the range of conceivable values and the constraint of these initial conditions are discussed. The differences between a blunt body wake and a slender body wake are discussed.

DD FORM 1 JAN 64 1473

UNCLASSIFIED

Security Classification

UNCLASSIFIED

Security Classification

14 KEY WORDS	LINK A		LINK B		LINK C	
	ROLE	WT	ROLE	WT	ROLE	WT
Turbulent wake Stratification Mixing model Initial turbulent intensity Mean centerline velocity						

INSTRUCTIONS

1. ORIGINATING ACTIVITY: Enter the name and address of the contractor, subcontractor, grantee, Department of Defense activity or other organization *(corporate author)* issuing the report.

2a. REPORT SECURITY CLASSIFICATION: Enter the overall security classification of the report. Indicate whether "Restricted Data" is included. Marking is to be in accordance with appropriate security regulations.

2b. GROUP: Automatic downgrading is specified in DoD Directive 5200.10 and Armed Forces Industrial Manual. Enter the group number. Also, when applicable, show that optional markings have been used for Group 3 and Group 4 as authorized.

3. REPORT TITLE: Enter the complete report title in all capital letters. Titles in all cases should be unclassified. If a meaningful title cannot be selected without classification, show title classification in all capitals in parenthesis immediately following the title.

4. DESCRIPTIVE NOTES: If appropriate, enter the type of report, e.g., interim, progress, summary, annual, or final. Give the inclusive dates when a specific reporting period is covered.

5. AUTHOR(S): Enter the name(s) of author(s) as shown on or in the report. Enter last name, first name, middle initial. If military, show rank and branch of service. The name of the principal author is an absolute minimum requirement.

6. REPORT DATE: Enter the date of the report as day, month, year, or month, year. If more than one date appears on the report, use date of publication.

7a. TOTAL NUMBER OF PAGES: The total page count should follow normal pagination procedures, i.e., enter the number of pages containing information.

7b. NUMBER OF REFERENCES: Enter the total number of references cited in the report.

8a. CONTRACT OR GRANT NUMBER: If appropriate, enter the applicable number of the contract or grant under which the report was written.

8b, 8c, & 8d. PROJECT NUMBER: Enter the appropriate military department identification, such as project number, subproject number, system numbers, task number, etc.

9a. ORIGINATOR'S REPORT NUMBER(S): Enter the official report number by which the document will be identified and controlled by the originating activity. This number must be unique to this report.

9b. OTHER REPORT NUMBER(S): If the report has been assigned any other report numbers *(either by the originator or by the sponsor)*, also enter this number(s).

10. AVAILABILITY/LIMITATION NOTICES: Enter any limitations on further dissemination of the report, other than those imposed by security classification, using standard statements such as:

(1) "Qualified requesters may obtain copies of this report from DDC."

(2) "Foreign announcement and dissemination of this report by DDC is not authorized."

(3) "U. S. Government agencies may obtain copies of this report directly from DDC. Other qualified DDC users shall request through

_____."

(4) "U. S. military agencies may obtain copies of this report directly from DDC. Other qualified users shall request through

_____."

(5) "All distribution of this report is controlled. Qualified DDC users shall request through

_____."

If the report has been furnished to the Office of Technical Services, Department of Commerce, for sale to the public, indicate this fact and enter the price, if known.

11. SUPPLEMENTARY NOTES: Use for additional explanatory notes.

12. SPONSORING MILITARY ACTIVITY: Enter the name of the departmental project office or laboratory sponsoring *(paying for)* the research and development. Include address.

13 ABSTRACT: Enter an abstract giving a brief and factual summary of the document indicative of the report, even though it may also appear elsewhere in the body of the technical report. If additional space is required, a continuation sheet shall be attached.

It is highly desirable that the abstract of classified reports be unclassified. Each paragraph of the abstract shall end with an indication of the military security classification of the information in the paragraph, represented as *(TS)*, *(S)*, *(C)*, or *(U)*.

There is no limitation on the length of the abstract. However, the suggested length is from 150 to 225 words.

14 KEY WORDS: Key words are technically meaningful terms or short phrases that characterize a report and may be used as index entries for cataloging the report. Key words must be selected so that no security classification is required. Identifiers, such as equipment model designation, trade name, military project code name, geographic location, may be used as key words but will be followed by an indication of technical context. The assignment of links, rules, and weights is optional.

Security Classification

Prepared for:

OFFICE OF NAVAL RESEARCH
Arlington, Virginia 22217

Scientific Officer:
Ralph D. Cooper
Program Director Fluid Dynamics

Approved: L. A. Hromas

L. A. Hromas, Manager
Fluid Mechanics Laboratory

TRW Systems Group
Redondo Beach, California

FOREWORD

This research was supported by the Advanced Research Projects Agency of the Department of Defense and was monitored by the Office of Naval Research, Ralph D. Cooper, Scientific Officer, under Contract N00014-72-C-0074. The work reported herein was performed by D. R. S. Ko, Flow Research, Inc., under TRW Subcontract No. 01OCH3E.

SUMMARY

The growth and collapse of the turbulent wake behind a submarine in a stratified ocean is studied analytically using simple phenomenological models. The present analysis closely follows the previous integral approach of Ko, based on the concept of local similarity and turbulent entrainment. A non-uniform entrainment rate, obtained by considering the three turbulent velocity components separately, marks the main difference to the previous approach. However, the present analysis is still limited to a wake without swirl and does not include the energy leakage through the internal wave field.

A series of parametric studies have been performed to study the effects of various operational conditions (such as stratification and speed) as well as the initial conditions on the wake flow field.

The solutions were found to be sensitive to some initial conditions. The physical significance, the range of conceivable values, and the constraints of these initial conditions are discussed. The differences between a blunt body wake and a slender body wake are pointed out, based on these parametric studies.

A comparison with the experiment of Schooley and Stewart is presented. Again, an extremely high initial turbulent intensity and degree of mixing are needed in the calculation. In addition to the fact that the body is practically a blunt one, it seems to suggest that an excessive amount of energy (more than required to balance the body drag for maintaining a uniform speed) may have been imparted to the wake. A much different result is expected from the wake of a slender, submarine-like body.

CONTENTS

LIST OF FIGURES

1. Introduction

Our understanding on the growth and collapse of the turbulent wake behind a submarine moving at a constant speed through a stratified medium has been vastly improved in recent years. The simplified integral analysis of Ko (ref. 1) has provided a general characterization of the various physical mechanisms associated with this complicated flow phenomenon. However, quite a few assumptions and approximations in that simplified analysis were understood to be unsatisfactory to provide a reliable prediction. Therefore, an improved analysis is presented here with the hope of arriving at a reliable first order prediction tool as well as enhancing our physical understanding of the submarine wake.

In the present analysis, the background ocean is assumed to be "quiet" which precludes the consideration of the ocean turbulent diffusion dominated far wake region. (reference 2 gives a general consideration of the diffusion of passive scalars behind a submarine in that particular region). Furthermore, no net momentum, either in the form of a swirl or a lift, is assumed to be imparted to the wake in the present analysis. These additional submarine motion associated effects will be considered after the present basic model being established.

2. Technical Approach and Formulation

The present analysis closely follows the previous integral approach of Ko (ref. 1) based on the concept of local similarity and turbulent entrainment. The main advantage of the integral approach over a finite difference approach is the simplicity in application to provide a quick appraisal of the various physical mechanisms associated with the submarine wakes. The shortcoming of such an approach is the inability in predicting the details as well as in giving a true representation of the region very close to the body where a highly non-similar flow field is expected.

The basic flow field of interest is shown schematically in Figure 1. The undisturbed medium outside the wake is assumed to be horizontally stratified with the density given by

$$\rho_o = \bar{\rho}\ (1-\alpha z) \tag{1}$$

with α being a constant. The corresponding density distribution inside the wake is taken to be

$$\rho_i = \bar{\rho}\ (1-\beta z) \tag{2}$$

with β being a variable equivalent density gradient. In the integral sense, the wake boundary is again assumed to be sharp and encloses all the anamolies in either density, turbulence or other wake identifying quantities (such as dye). The possible differences between a dye wake and others will not be considered here.

It is again assumed that there is no direct effect of turbulence on the inviscid flow field in the cross plane. The effect of turbulence is being accounted for through the moving boundary and the equivalent local density gradient. Therefore, as derived in Reference 1, with the locally similar velocity distribution

$$\begin{aligned} \bar{v} &= y f_1(x) \\ \bar{w} &= -z f_1(x) \end{aligned} \tag{3}$$

the wake boundary can be shown to remain elliptical at all times and is given by

$$\frac{y^2}{a^2} + \frac{z^2}{b^2} = 1 \tag{4}$$

with a and b representing the major and the minor axis. Furthermore, using the assumption of external pressure field remaining hydrostatic, the cross plane momentum equations lead to a governing equation for the "rate of collapse" f_1

$$U_o \left(1 + \frac{b^2}{a^2}\right) \frac{df_1}{dx} = \frac{b^2}{a^2} (\alpha-\beta)\, g - \left(1 - \frac{b^2}{a^2}\right) f_1^2 \tag{5}$$

The concept of turbulent entrainment of the outer fluid leads to the following governing equations for the rate of change of the wake boundaries

$$\begin{aligned} U_o \frac{da}{dx} &= af_1 + E_y(x) \\ U_o \frac{db}{dx} &= -bf_1 + E_z(x) \end{aligned} \tag{6}$$

where E_y and E_z represent the entrainment velocities in the y and z directions at the wake boundary $y = a$ and $z = b$. The previous analysis assumes a more or less uniform entrainment rate by linking the entrainment velocities to the local total turbulent intensity level. This approximation is definitely undesirable in the expectation that only the vertical entrainment rate is inhibited by the effect of stratification. Therefore, an intrinsically non-uniform entrainment rate is assumed here by letting

$$\begin{aligned} E_y &= K_1 v_m' \\ E_z &= K_1 w_m' \end{aligned} \tag{7}$$

with v_m' and w_m' denoting the averaged rms turbulent velocity components in the y and z directions. Then, the rate of area increase is given by

$$\frac{U_o}{A} \frac{dA}{dx} = K_1 \left(\frac{v_m'}{a} + \frac{w_m'}{b}\right) \tag{8}$$

Turbulent Energy Equations

Instead of using an overall turbulent energy equation, three separate energy equations, one for each velocity component, are used to account for the anisotropy expected in a stratified flow. The governing equations with appropriate simplifications can be written in the following forms:

$$\frac{1}{2}\frac{D}{Dt}\overline{u'^2} = -\overline{u'v'}\frac{\partial\bar{u}}{\partial y} - \overline{u'w'}\frac{\partial\bar{u}}{\partial z} - \frac{1}{\bar{\rho}}\overline{u'\frac{\partial p'}{\partial x}} - \varepsilon'$$

$$\frac{1}{2}\frac{D}{Dt}\overline{v'^2} = -\overline{v'^2}\frac{\partial\bar{v}}{\partial y} - \overline{v'w'}\frac{\partial\bar{v}}{\partial z} - \frac{1}{\bar{\rho}}\overline{v'\frac{\partial p'}{\partial y}} - \varepsilon' \qquad (9)$$

$$\frac{1}{2}\frac{D}{Dt}\overline{w'^2} = -\overline{v'w'}\frac{\partial\bar{w}}{\partial y} - \overline{w'^2}\frac{\partial\bar{w}}{\partial z} - \frac{1}{\bar{\rho}}\overline{w'\frac{\partial p'}{\partial z}} - \varepsilon' - \frac{g}{\bar{\rho}}\overline{\rho'w'}$$

where ε' denotes the viscous dissipation terms and

$$\frac{D}{Dt} = \bar{u}\frac{\partial}{\partial x} + \bar{v}\frac{\partial}{\partial y} + \bar{w}\frac{\partial}{\partial z}$$

A few interesting features can be immediately observed from equations (9).

(a) Except for flow with an appreciable mean swirl, the production terms effectively appears in the equation for $\overline{u'^2}$ only. The exchange of energy with the mean flow is mainly carried out through the axial component.

(b) The pressure velocity correlation terms, which serve the function of redistributing the available energy among the three components in an attempt to achieve isotropy, cancel each other in the governing equation for the total turbulent energy

$$e' = \frac{1}{2}(\overline{u'^2} + \overline{v'^2} + \overline{w'^2})$$

(c) The effect of stratification, with the Boussinesq approximation, appears in the governing equation for $\overline{w'^2}$ only.

The modelling of each term is briefly discussed in the following:

Production

The simple concept of an eddy viscosity is felt to be adequate for the present purpose. It is assumed that

$$- \overline{u'w'} \sim \varepsilon_z \frac{\partial \bar{u}}{\partial z}$$

$$- \overline{u'v'} \sim \varepsilon_y \frac{\partial \bar{u}}{\partial y} \tag{10}$$

The eddy viscosities are then related to the corresponding turbulent intensity and integral length scale by

$$\varepsilon_y = K_e' \lambda_y (\overline{v'^2})^{\frac{1}{2}}$$

$$\varepsilon_z = K_e' \lambda_z (\overline{w'^2})^{\frac{1}{2}} \tag{11}$$

These eddy viscosities are further assumed to be constant across the wake but changing in the axial direction. The anisotropic nature of a stratified flow is built into Equation (11). The eddy viscosity constant K_e' will be further discussed in a later section.

Dissipation

The modelling of the energy dissipation term follows the same argument of Townsend (ref. 3) but equally distributed among the three components. Specifically,

$$\varepsilon' = - \frac{1}{2} \frac{d}{dt} \overline{u'^2}$$

then,

$$\varepsilon' \simeq \frac{1.1}{2} \frac{u'^3}{\lambda} = 0.3 \frac{e'^{3/2}}{\lambda} \tag{12}$$

Here λ denotes the integral length scale which will be taken to be the geometrical average of λ_y and λ_z i.e.,

$$\lambda = (\lambda_y \lambda_z)^{\frac{1}{2}} \tag{13}$$

Pressure Velocity Correlation

The pressure velocity correlation terms are modelled after Rotta (ref. 4) which gives

$$\overline{p' \left(\frac{\partial u_i'}{\partial x_k} + \frac{\partial u_k'}{\partial x_i} \right)} = C_\phi \bar{\rho} \frac{\sqrt{2e'}}{\lambda} \left(\frac{2e'}{3} \delta_{ik} - \overline{u_i' u_k'} \right) \tag{14}$$

where C_ϕ denotes an universal constant having a value of about 1.6 as suggested by the experimental data (refer to Hanjalic and Launder (ref. 5) but noted that some algebraic manipulations are required to arrive at the above expression).

Stratification

The effect of stratification is also included using a turbulent eddy diffusivity model, which gives

$$-\overline{\rho' w'} \sim \varepsilon_\rho \frac{\partial \rho_i}{\partial z} \tag{15}$$

Furthermore, assuming the turbulent Schmidt number in the vertical direction to be unity, we have

$$\varepsilon_\rho = \varepsilon_z \sim \lambda_z (\overline{w'^2})^{\frac{1}{2}} \tag{16}$$

Using these simple modellings, the three governing equations (9) can be readily integrated across the wake. Let's define the area averaged turbulent energy in the three principal directions by

$$\begin{aligned} u_m'^2 \, A &= \frac{1}{2} \int_A \overline{u'^2} \, dA \\ v_m'^2 \, A &= \frac{1}{2} \int_A \overline{v'^2} \, dA \\ w_m'^2 \, A &= \frac{1}{2} \int_A \overline{w'^2} \, dA \end{aligned} \tag{17}$$

and the total area averaged turbulent energy by

$$e = u_m'^2 + v_m'^2 + w_m'^2 \tag{17a}$$

The integral governing equations become

$$U_o \frac{d}{dx}(u_m'^2 A) = K_p A U_d^2 \left(\frac{v_m'}{a} + \frac{w_m'}{b}\right) + C_p \frac{\sqrt{2e}}{\Lambda} A \left(\frac{2e}{3} - 2u_m'^2\right) - 0.3A \frac{e^{3/2}}{\Lambda} \tag{18a}$$

$$U_o \frac{d}{dx}(v_m'^2 A) = -2f_1 v_m'^2 A + C_p \frac{\sqrt{2e}}{\Lambda} A \left(\frac{2e}{3} - 2v_m'^2\right) - 0.3A \frac{e^{3/2}}{\Lambda} \tag{18b}$$

$$U_o \frac{d}{dx}(w_m'^2 A) = 2f_1 w_m'^2 A + C_p \frac{\sqrt{2e}}{\Lambda} A \left(\frac{2e}{3} - 2w_m'^2\right)$$
$$- 0.5A \frac{e^{3/2}}{\Lambda} - \frac{K_\rho}{2} A w_m' \beta g b \qquad (18c)$$

where Λ = the integral length scale on the wake axis. $\Lambda = C_i (ab)^{\frac{1}{2}}$ in the present model with $C_i = 0.125$.

C_p : the pressure-velocity correlation coefficient which is related to C_ϕ and is estimated to be $C_p = 0.8$.

K_ρ : $K_\rho = \frac{\epsilon_\rho}{b w_m'} = 0.18$

K_p : an integrated constant in the production term related to the eddy diffusivity constant K_e', and with some assistance of the experimental data, we have $K_p = 0.12$.

The quantity U_d represents the maximum mean velocity excess on the wake axis. In the previous analysis, a correlation obtained by Naudascher (ref. 6) was used to relate this quantity to the local turbulent intensity. However, this correlation of Naudascher seems to be unique to that particular experiment and is believed to be a weak link in the previous analysis. In order to have a better assessment of the energy production term, it is decided to leave U_d as a variable to be governed by the mean centerline axial momentum equation.

Let's assume the mean axial velocity field to be given by

$$\bar{u} = U_o + U_d F\left(\frac{y}{a}, \frac{z}{b}\right) \qquad (19)$$

The mean centerline axial momentum equation gives

$$U_o \frac{dU_d}{dx} = -\left(\frac{1}{\rho}\frac{\partial p}{\partial x}\right)_o + K_\epsilon U_d \left(\frac{v_m'}{a} + \frac{w_m'}{b}\right) F'' \qquad (20)$$

where F'' denotes the curvature of the mean velocity profile on the wake axis and K_ϵ is the eddy viscosity constant defined by

$$\epsilon_y = K_\epsilon v_m' a \quad , \quad \epsilon_z = K_\epsilon w_m' b \qquad (21)$$

The pressure gradient term is included to account for the small pressure gradient field induced by the collapsing motion, which can be easily evaluated.

For the case of a momentumless wake and zero axial pressure gradient, it can be easily shown that

$$U_d A^2 \simeq \text{constant} \tag{22}$$

Using eqn. (8), the entrainment constant K_1 is readily given by

$$K_1 = 0.5\, K_\varepsilon\, F'' \tag{23}$$

Using $K_\varepsilon = K_\rho = 0.18$ and the experimentally measured value of $F'' \cong 25$, the entrainment constant can be estimated to be $K_1 = 2.25$. This value agrees fairly well with the growth rate obtained in Naudascher's experiment.

Mixing Model

Because of the use of a global entrainment concept and an equivalent internal density gradient, any attempt to derive a mixing equation is not likely to arrive at a consistent result which can properly account for the effect of turbulence on the mixing process inside the wake. For that reason, we have decided to use a phenomenological model to obtain a governing equation for the density gradient β inside the wake.

First of all, the total potential energy inside the wake is given by

$$V = \frac{\pi \bar{\rho} g U_o}{8} \frac{(\alpha-\beta)^2}{\alpha} ab^3 \tag{24}$$

Therefore, this equivalent linear density gradient β may be considered as an averaged quantity which provides a measure of the available potential energy inside the wake at any given station. By assuming that the potential energy per unit area in the wake is directly proportional to the available turbulent energy per unit area in the direction against the gravitational field, the governing equation for β can be written as

$$\beta b = \alpha b - (\alpha-\beta_o) b_o \frac{w'_m}{w'_{mo}} \tag{25}$$

It should be noted that this model actually is not applicable to any premixed region, such as the laminar experiment of Wu (ref. 7).

Nondimensionalization

Following the same nondimensionalization procedure of reference 1, the following characteristic quantities are used:

Characteristic length	L = initial wake size
Characteristic velocities	U_o = sub speed
	$U_{ref} = e_o^{1/2}$ = initial turbulent intensity
Characteristic time	$N^{-1} = (\alpha g)^{-1/2}$

Furthermore, using the asterik to denote the nondimensional quantities, the following eight dependent variables are defined by

$a^* = a/L$, $b^* = b/L$	Wake dimensions
$f_1^* = f_1/N$	Collapsing rate
$u_m^* = u_m'/U_{ref}$	
$v_m^* = v_m'/U_{ref}$	Turbulent velocities
$w_m^* = w_m'/U_{ref}$	
$\beta^* = \beta L$	Internal density gradient
$U_d^* = U_d/U_o$	Mean centerline axial velocity excess

The problem is then reduced to finding the variation of these unknowns, which describe the wake evolution, as functions of a nondimensional distance defined by

$$x^* = \frac{xN}{U_o} = \frac{x}{D}\frac{1}{F_r} \tag{26}$$

where $F_r = \frac{U_o}{ND}$, the Froude number based on the body diameter, D and the free-stream velocity, U_o. These unknown quantities are governed by the following set of first order ordinary differential equations:

Entrainment

$$\frac{da^*}{dx^*} = a^* f_1^* + K_1 F_t v_m^* \tag{27a}$$

$$\frac{db^*}{dx^*} = -b^* f_1^* + K_1 F_t w_m^* \tag{27b}$$

Cross plane momentum

$$(1 + \frac{b^{*2}}{a^{*2}}) \frac{df_1^*}{dx^*} = (1 - \frac{\beta^*}{\alpha^*}) \frac{b^{*2}}{a^{*2}} - (1 - \frac{b^{*2}}{a^{*2}}) f_1^{*2} \tag{27c}$$

Turbulent Energy

$$\frac{d}{dx^*}(u_m^{*2} a^* b^*) = K_p \frac{F_t}{U_N^2} a^* b^* U_d^{*2} (\frac{v_m^*}{a^*} + \frac{w_m^*}{b^*}) - 0.3 F_t \frac{e^{*3/2} a^* b^*}{\Lambda^*}$$

$$+ C_p \frac{\sqrt{2e^*}}{\Lambda^*} a^* b^* F_t (\frac{2e^*}{3} - 2u_m^{*2}) \tag{27d}$$

$$\frac{d}{dx^*}(v_m^{*2} a^* b^*) = -2 f_1^* v_m^{*2} a^* b^* + C_p \frac{\sqrt{2e^*}}{\Lambda^*} a^* b^* F_t (\frac{2e^*}{3} - 2v_m^{*2})$$

$$- 0.3 F_t \frac{e^{*3/2} a^* b^*}{\Lambda^*} \tag{27e}$$

$$\frac{d}{dx^*}(w_m^{*2} a^* b^*) = 2 f_1^* w_m^{*2} a^* b^* + C_p \frac{\sqrt{2e^*}}{\Lambda^*} a^* b^* F_t (\frac{2e^*}{3} - 2w_m^{*2})$$

$$- 0.3 F_t \frac{e^{*3/2} a^* b^*}{\Lambda^*} - \frac{K_\rho}{2} \frac{1}{F_t} (\frac{\beta^*}{\alpha^*}) w_m^* a^* b^{*2} \tag{27f}$$

Mixing

$$\frac{d}{dx^*}(\beta^* b^*) = \alpha^* \frac{db^*}{dx^*} - \frac{(\alpha^* - \beta_o^*) b_o^*}{w_{mo}^*} \frac{dw_m^*}{dx^*} \tag{27g}$$

Mean centerline axial momentum

$$\frac{dU_d^*}{dx^*} = -2K_1F_tU_d^*\left(\frac{v_m^*}{a^*}+\frac{v_m^*}{b^*}\right)-\frac{1}{2}\left(\frac{U_N}{F_t}\right)^2\frac{d}{dx^*}\left[\frac{b^{*2}\left\{2f_1^{*2}+(1-\beta^*/\alpha^*)(1-b^{*2}/a^{*2})\right\}}{1+b^{*2}/a^{*2}}\right] \quad (27h)$$

It is clear from these equations that two nondimensional parameters govern the solutions: the turbulent Froude Number F_t defined by

$$F_t = \frac{U_{ref}}{NL} \quad (28a)$$

and the initial turbulent intensity parameter U_N given by

$$U_N = \frac{U_{ref}}{U_o} \quad (28b)$$

The turbulent Froude number is related to the ordinary Froude number by

$$F_t = U_N\left(\frac{D}{L}\right)F_r \quad (28c)$$

The solutions to this set of ordinary different equations can be obtained numerically with a prescribed set of initial conditions at $x^* = x_o^*$. In fact, instead of appearing explicity in the governing equations, a few fundamental parameters to this problem are hidden in the form of initial conditions. Therefore, a full discussion of the physical significance, the proper choice of values and the constraints on the initial conditions is given in the following:

Initial Conditions

(a) a_o^*, b_o^* Initial wake dimension. With the initial wake dimension L being chosen for normalization, both a_o^* and b_o^* can be set equal to one if the wake is assumed to be circular initially. However, experimental observations have indicated a relatively strong stratification effect on the initial wake aspect ratio (b_o^*/a_o^*), the effect on the overall solution will have to be studied parametrically.

(b) f_{10}^* Initial rate of collapse. Assuming that the fluid particles do not possess an initial velocity field in the cross plane, the initial value of f_{10}^* can be readily set as zero. A parametric study is again required to assess its significance on the solution.

(c) u_{mo}^*, v_{mo}^*, w_{mo}^* Initial anisotropy. Using $e_o^{1/2}$ as the reference quantity, it requires $u_{mo}^{*2} + v_{mo}^{*2} + w_{mo}^{*2} = e_o^* = 1$ Thus, the relative magnitude of these quantities represents the initial degree of anisotropy. For an initially isotropic turbulent field, $u_{mo}^{*2} = v_{mo}^{*2} = w_{mo}^{*2} = \frac{1}{3}$

(d) U_{do}^* Initial mean axial velocity excess. For a wake of zero net axial momentum, this value represents the amount of mean energy flux remaining in the wake at the initial station.

(e) β_o^* Initial mixing effectiveness. This quantity measures the initially available potential energy in the wake. A combination of β_o^* and f_{10}^*, gives the total initial energy being imparted to the wake which is expected to control, to a large extent, the collapse process. Since little is known about the degree of initial mixing, it is decided to set $f_{10}^* \equiv 0$ in the present report in order to simplify the discussion.

At this point, we seem to be facing a large number of possible combinations of parameters and the proper choice of values becomes extremely critical in assessing the potential utility of such an analysis. It is worthy to note that this is exactly the primary goal of this type of simple integral approach to bring out the important physical variables and governing parameters in a complex flow. A sensitivity study of these parameters must be performed in order to identify their relative significance to the solutions. Existing experimental data provide a reasonable estimate on a few parameters, but additional experimental information is required in order to obtain a reliable selection of the initial conditions for future application. On the other hand, these initial conditions can not be arbitrarily assigned even though the governing equations may not have posed any restriction on the values. The physical constraints on the initial conditions, based mainly on energy consideration, are briefly discussed in the following.

Constraints on the initial conditions

(a) Experimental data shows that at an initial station where appreciable mean shear still exists, $\frac{u'_{max}}{U_d} \sim 0(1)$. For a Gaussian distribution, the maximum axial turbulent velocity intensity can be related to the area averaged total turbulent intensity by $e^{\frac{1}{2}} = 0.625\ u'_{max}$. Hence, at an initial station not too far downstream from the body where the momentumless nature becomes important, the initial mean axial velocity excess is related to the initial turbulent intensity by

$$U_{do}^{*} \sim K\ U_N \tag{29}$$

with K being about 2. As discussed previously, this constant K may be different if excessive energy still remains in the mean flow at the initial station. To some extent, this "constant" K should depend on the configuration in achieving a flow with no net axial momentum. For example, Naudascher's type experiment with the thrust being supplied by a jet is expected to have more residual mean energy as compared with a propeller driven body. Additional consideration and more experimental information are required to provide a better estimate of the relative energy content in the mean and in the turbulent field. For the present purpose, the crude estimate of K = 2 is used and a sensitivity study will be performed and discussed in the next section.

(b) The initial total turbulent energy flux is given by

$$E_{to} = \rho U_o U_{ref}^{2} A_o$$

On the other hand, for a body moving at an uniform speed U_o, the total energy imparted to the wake can be written as

$$E_{drag} = U_o(\text{Drag})$$

$$= \frac{1}{2} \rho U_o^{3} C_D A_b$$

where C_D is the drag coefficient of the body based on the frontal area A_b. Then the percentage of energy goes into turbulence is given by

$$\frac{E_{to}}{E_{drag}} = \frac{8}{C_D} U_N^2 \left(\frac{L}{D}\right)^2 \tag{30}$$

A typical number of 10 $\sim$20% would be reasonable for a slender body wake without extraneous energy sources. Therefore, the values of U_N can not be chosen arbitrarily. It is also interesting to note that an appreciable difference in the magniture of U_N is expected between a slender body wake and a blunt body wake because of the difference in C_D. In addition, the ratio of the total turbulent energy to the total energy input can also depend on the body configuration which makes the choice of U_N quite different for blunt and slender body wakes. Further discussions will be given in the next section.

(c) The total initial potential energy flux can be written as

$$V_o = \frac{\bar{\rho} g U_o}{8} \frac{(\alpha-\beta_o)^2}{\alpha} A_o b_o^2$$

Then,

$$\frac{V_o}{E_{drag}} = \frac{1}{C_D} \left(\frac{L}{D}\right)^4 F_r^{-2} \left(1 - \frac{\beta_o}{\alpha}\right)^2 \tag{31}$$

Again, this ratio poses a lower bound for the conceivable values of (β_o/α). We don't really have a good estimate on the percentage of available energy appearing in the form of a potential energy. However, it must satisfy the inequality.

$$\frac{V_o}{E_{drag}} < 1 - \frac{E_{to}}{E_{drag}} - \frac{E_{mean}}{E_{drag}} \tag{32}$$

where E_{mean} indicates the energy associated with the mean flow at the initial station. It may also be noted that C_D again plays an important role as well as the Froude number.

3. Results and Discussions

3.1 Nonstratified Wakes

As a check for the empirical constants used in the present analysis, a calculation has been made for a momentumless wake in a homogeneous medium. The initial conditions at x/D = 5 were taken from a recent wind tunnel experiment of Gran (ref. 8). Since the data is still being reduced at the present time, no specific comparison is shown here. Figure 2 shows the growth of the wake radius as a function of (x/D). Approximately $r^* \sim x^{0.25}$ which agrees well with the preliminary data of Gran as well as some recent FRI towing tank data by Pao et al. (ref. 9)

Figure 3 shows the decay of the mean centerline axial velocity excess which follows a nearly x^{-1} law. This is certainly consistent with the wake growth rate for a momentumless wake. Preliminary data of Gran shows a similar decay while a much faster decay rate ($\sim x^{-2}$) was indicated by Naudascher. It is generally agreed that the mean flow measurements of Naudascher are not consistent with the other turbulent measurements. Therefore, we feel that the consistency with the momentumless nature of the flow, which is exhibited by the present solution, is more important and the disagreement with Naudascher's mean flow data will be ignored. Figure 4 gives the decay of the turbulent intensity u_m^*, which shows a nearly x^{-1} dependence. This decay rate is in reasonable agreement with Naudascher but seems to be slightly faster than the measurements of Gran. However, as noted in this figure, the decay rate is slowing down at increasing x/D, and the no-swirl assumption of the present analysis should account for part of the faster decay of the turbulent intensity.

In summary, the calculations for the nonstratified wake has provided enough confidence on the numerical constants used in the present analysis and the remaining section will be dealing with the stratified wakes only using these prefixed constants.

3.2 Typical Results

Figure 5 shows a typical calculated variations of the wake height (b^*) and width (a^*) as a function of the nondimensional distance x^* for

$$F_r = \frac{U_o}{NL} = 10$$

$$U_N = e_o^{1/2}/U_o = 0.1$$

$$\beta_o/\alpha = 0.5$$

The results indicate that the wake, initially circular, grows nearly axisymmetrically before reaching a maximum height and then "collapses". The general characters of the solution remains the same as the results of the previous analysis (ref. 1). The phenomenon of "over collapse" seems to remain which is partially caused by not including the internal wave energy losses.

It is more interesting to note the decay of the three turbulent components which is shown on Figure 6. The calculations were performed by assuming an equipartician of the turbulent energy among the three modes. As seen in Figure 6, because of the mean shear production term, energy is fed into u_m^* initially. Then the stratification effect appears and starts to take energy away from w_m^*. The tendency toward isotropy term is not powerful enough to compensate for the energy gain by u_m^* and the energy drain by w_m^*. Therefore, an anisotropic turbulence field is developed. In fact, at some distance beyond the point of collapse, the turbulence becomes essentially two dimensional with nearly equal amounts of energy in the u' and the v' components. In the present entrainment model, the vertical entrainment is practically shut-off while the horizontal entrainment continues. This fact is reflected in Figure 7 where the wake area is plotted against x^*. In the previous model, an asymptotic area is reached at a short distance beyond the point of collapse.

3.3 Effect of initial anisotropy

The initial turbulence field is expected to possess a certain degree of anisotropy either as a result of the stratification effect on the body boundary layer or caused by the propeller. The effect of these initial anisotropy on the flow has been studied by setting $u_{mo}^{*2}: v_{mo}^{*2}: w_{mo}^{*2}$ equal to 1:1:1, (the typical case studied above), 1:2:2 and 2:2:1. Except for a small difference in u_m^*, v_m^* and w_m^* at small x^*, the three sets of solution are almost indistinguishable from the results shown on Figures 5-7. Based on these findings, it is concluded that the initial anisotropy tends to be quickly removed by the tendency toward isotropy terms. Thus, with the exception of a strongly stratified environment, the effect of anisotropy on the wake evolution is small and an equipartician of the initial turbulent energy among three modes is assumed throughout the remaining calculations.

3.4 Effect of initial degree of mixing

As stated previously, the initial density gradient β_o represents a measure of the total amount of potential energy deposited in the wake. Therefore, its effect on the wake collapse is expected to be quite pronounced as demonstrated on Figure 8. Three sets of a^* and b^* are shown on Figure 8, for $\beta_o/\alpha = 0$ (perfectly mixed), 0.5, and 0.9 (poorly mixed). The results, though expected, are strikingly different. In particular, for $\beta_o/\alpha = 0.9$, the "collapse" is hardly "visible" with only the maximum wake height being limited. By defining the distance to collapse as x_c^* where $b^* = b^*_{max}$, it is easily observed that x_c^* increases rapidly with increasing β_o/α. This type of finding has been extensively used recently in a qualitative manner to explain the differences in the various experiments. It is interesting to note that the effect of initial mixing on the overall wake evolution is quite small as all three sets of solution curves give nearly the same growth rate of the wake area.

The variation of β/α is shown on Figure 9, for four different initial density gradients. It should be cautioned that this initial mixing parameter β_o is different from that used in the previous analysis, where the equivalent density gradient was kept at constant before collapse as shown in Figure 9 for the purpose of comparison.

The intermediate value of $\beta_o/\alpha = 0.5$ has been used for most of the parametric studies performed here. Some definitive measurements for the mixing effectiveness behind the full scale body are needed to provide a better estimate of the values to be used for prediction purpose. At this point, we can only note that for a slender body with $C_D = 0.2$, the potential energy deposited in the wake ranges from .05% to 5% of E_{drag} for the cases shown on Figures 8 and 9.

3.5 Effect of stratification and speed

The effects of stratification and speed can be grouped into a single parameter $F_r = \frac{U_o}{ND}$, the Froude number. Figure 10 shows the wake height variation for a range of Froude numbers. For fixed values of U_N and β_o/α, the maximum wake height increases with increasing F_r (faster body speed or weaker stratification). The nondimensional location of collapse, x_c^* also increases with increasing F_r. This is different from the previous analysis which gives x_c^* constant for a wide range of Froude number. Furthermore, the degree of

collapse (measured by the rate of collapse at the maximum height) decreases with increasing F_r. Since the nondimensional distance $x^* = \frac{X}{D}\frac{1}{F_r}$, the effect is much more evident in the physical coordinates as shown on Figure 11. The relative degree of collapse can be readily assessed in such a plot.

The explanation for the strong effect of Froude number can be obtained from Figure 12 where the normalized wake area is plotted against x^* for several Froude numbers. For increasing F_r, the relative effect of stratification is much weaker, the vertical entrainment becomes less restricted and more fluid is being entrained into the wake. The effect of Froude number on the decay of the mean centerline axial velocity is shown on Figure 13. The decay of U_d^* tends to slow down for increasing stratification (F_r decreases). This general behavior of the effect of stratification on the mean velocity decay has been observed experimentally by Pao et al. (ref. 9). A direct comparison will be performed in the future when more experimental data becomes available.

3.6 Effect of initial turbulent intensity

By keeping F_r equal to a constant ($F_r = 10$), Figure 14 shows the effect of U_N, the initial turbulent intensity level, on the wake height. The results are similar to the previously discussed effect of Froude number; with increasing U_N, $F_t = U_N F_r$ increases, b^*_{max} increases, x^*_c increases, and the degree of collapse slightly weakened. However, the interpretation is entirely different. First of all, there is no stretching of the physical distance x for the four different values of U_N. Therefore, their effect on the degree of collapse is relatively weaker. Secondly, as discussed in the previous section, the magnitude of U_N is a measure of the initial total turbulent energy. Also shown on the curves are the corresponding values of E_{to}/E_{drag} for each U_N. The body drag coefficient is purposedly left unspecified. For a slender body, the drag coefficient is expected to be about $0.1 \sim 0.2$. If the ratio E_{to}/E_{drag} is assumed to be of the order of $10 \sim 20\%$, a typical value of $U_N \simeq 0.05$ would have been reasonable for a slender body wake. On the other hand, $C_D \simeq 1$ for a blunt body. Thus, a higher value of U_N can be expected and its effect on the wake is clearly demonstrated on Figure 14. However, U_N can not be assigned arbitrarily as indicated by the curve for $U_N = 0.4$. Solution can still b obtained but more energy than available will have to be stored in the turbulent field even for a blunt body wake. This is certainly unrealistic unless some extraneous sources of energy have been introduced into the flow field.

3.7 Effect of integral scale length

Instead of using a separate length scale equation for the turbulent integral scale, an algebraic relationship between the integral length scale and the equivalent wake radius was used, i.e.

$$\Lambda = C_i (ab)^{\frac{1}{2}}$$

After searching through a limited amount of experimental information, the value of C_i was taken to be 0.125. The effect of this constant on the wake dimension is shown on Figure 15, for a $\pm$ 40% variation of C_i. It should be noted that this is only a qualitative assessment of the effect since the integral length scale only affects the dissipation and the pressure velocity correlation terms in this model. An increasing length scale implies a slower decay as shown on Figure 16 where the decay of turbulent energy level is plotted verses x^*. To be more rigorous, the effect of integral length scale on the energy production term, which has been absorbed in the constants here, must be included. This modification is expected to accentuate the effect.

It is also interesting to note that the experimental observations of Gran seems to indicate a larger C_i for a drag wake than a momentumless wake. The corresponding consequences of this difference may be inferred from these results.

3.8 Effect of initial mean velocity excess

The initial value of U_{do}^* gives a measure of the amount of energy remained in the mean flow. Since the transfer of energy from the mean to the turbulent field is relatively inefficient in a turbulent wake model, the effect on the wake solution is quite small as indicated on Figure 17 where two sets of curves are shown bounding four calculations for $U_{do}^* = 0.05, 0.1, 0.2$ and 0.3. The corresponding mean velocity decay is shown on Figure 18. This comparison points out that a crude estimate on the initial value of U_{do}^* is quite adequate except for the prediction of U_d^*.

3.9 Effect of initial wake geometry

There are at least two reasons for the initial wake geometry to be non-circular as assumed so far. First of all, the basic body geometry is not exactly axisymmetric and small angle of attack can have a strong influence on the initial wake shape for a slender body. Secondly, the effect of stratification on the body boundary layer is expected to limit the vertical growth. Hence, a larger aspect ratio, a/b is expected with increasing stratification. This

dependence of the initial wake geometry on stratification has been observed qualitatively by Pao et al. (ref. 9); and its effect on subsequent wake development must be explored.

Figure 19 shows the effect of the initial wake geometry on the downstream wake evolutions. The initial area is kept at constant for the three cases. The effect on the total wake area variation is quite small. However, the effect on the apparant wake collapse is surprisingly strong. Practically no collapse in the classical sense can be stated for the case 2. On the other hand, a much stronger collapse at a smaller x_c^* occurs for the case 3 where $(b/a)_o > 1$. This result provides a partial explanation to the much weaker collapse being observed recently in comparison with the previous experiment of Schooley and Stewart (ref. 10) who used a fairly blunt body, for which a more or less circular initial wake shape was expected. Additional discussions on the experiment of Schooley and Stewart will be given in the following.

3.10 Experiment of Schooley and Stewart

In the previous report of Ko, a comparison with the laboratory experiment of Schooley and Stewart was presented. Extraordinary high initial turbulent intensity ($U_N = 0.45$) was required to match the initial wake growth and the maximum wake height observed in the experiment. It is worthy to note that since the averaged value is used in this type of integral analysis, a much higher local maximum intensity is expected. For $U_N = 0.45$, with a Gaussian distribution, we have

$$\frac{u'_{max}}{U_o} = 0.72$$

a nonrealistically high value. Therefore, an attempt to use the present analysis, together with the understanding achieved through the parametric studies, to compare with and to interpret the results of Schooley and Stewart is given here.

The flow conditions for the experiment are:

$$N = 2.19 \text{ sec}^{-1}$$

$$U_o = 45 \text{ cm/sec}$$

$$L = 3 \text{ cm}$$

$$F_r = \frac{U_o}{NL} = 6.8$$

A larger initial wake dimension L was chosen with the hope of getting slightly farther away from the body where a complicated flow field is expected from the relatively large propeller. With a body of aspect ratio (length to diameter) 2, it is practically a blunt body wake. Figure 20 shows a comparison of the calculation using

$$U_N = 0.3$$

$$F_t = 2.0$$

$$\beta_o/\alpha = 0.15$$

As indicated on the figure, this initial turbulent intensity level corresponds to $E_{to}/E_{drag} = 1.3/C_D$. Even with $C_D = 1$ for a blunt body wake, the number is still non-realistic unless additional work or energy input has been required to propell the body. The possibility of additional drag on the guided wires and the non-constant velocity nature of the test can not be discounted. All these comparisons tend to point out that the experiment of Schooley and Stewart, though being extremely instructive in demonstrating the wake collapse phenomenon, is quite far from simulating a typical submarine wake. For the purpose of illustration, a calculation, assuming the body were streamlined and sub-like, is presented on the same graph. The dramatic difference in the wake development can explain, to a large extent, the inconsistency of the recent laboratory experiments with the previous observations of Schooley and Stewart.

4. Summary and Concluding Remarks

An improved phenomenological model has been developed for studying the turbulent wake behind a submarine moving with a uniform speed in a linearly stratified quiet ocean. Based on a series of parametric studies, the following conclusions are reached:

(a) Initial anisotropy has a small effect on the wake unless an unusually strong stratification is encountered. Therefore, the initial turbulent field may be assumed as isotropic for most practical situations.

(b) Because of the stable stratification, the vertical turbulence component becomes vanishingly small after the wake reaches a maximum height and the turbulence field becomes essentially two-dimensional.

(c) The initial degree of mixing (β_o) has an appreciable effect on the "degree of collapse" as well as the location of collapse but it has relatively small effect on the other flow variables.

(d) The maximum wake height increases with increasing initial turbulence level U_N. Also, the location of collapse, x_c^*, increases with increasing U_N. The choice of U_N must be consistent with the energy consideration and depends on the body configuration.

(e) The effect of the initial mean centerline velocity excess is quite small on the general flow field. A reasonable choice is $U_{do}^* = 2\ U_N$.

(f) Increasing integral length scale slows down the turbulent decay and therefore increases entrainment. Since a drag wake is expected to have a larger integral length scale than a momentumless wake, a larger b_{max}^* is expected for a drag wake.

(g) Stratification and speed effects on the wake is scaled by the Froude number defined by $F_r = \frac{U_o}{NL}$. For increasing F_r, b_{max}^* increases, the physical distance to collapse increases and the degree of collapse lessens.

(h) A "pre-collapsed" wake, either caused by the stratification effect on the body boundary layer or by the body geometry, has a strong effect on the degree of collapse.

(i) A blunt body wake is expected to behave quite differently from a slender body sub-like wake because of:

- initial turbulent intensity
- initial degree of mixing
- initial wake geometry

(j) The experiment of Schooley and Stewart is atypical as compared to a sub-like body wake. Furthermore, excessive drag or energy input seems to be deposited into the wake based on the present investigation.

These conclusions are tentative in nature, more parametric studies and comparison with available laboratory experiments are required to better assess these conclusions. The energy leakage through the internal wave field must be included in the future. This coupling with the internal wave field should avoid the overcollapse phenomenon. Furthermore, no swirl has been included in the analysis. In reality, a certain amount of swirl is deposited in the wake. The effects of swirl will have to be investigated before the model can be used with confidence. A future report will be dealing specifically with these points.

References

(1) Ko, D.R.S., "Collapse of a turbulent wake in a stratified medium", TRW Report 18202-6001-RO-00, Vol. II, November, 1971.

(2) Ko, D.R.S. and Alber, I.E., "Diffusion of a passive scalar", TRW Report 20086-6001-RO-00, February, 1972.

(3) Townsend, A.A., "The structure of turbulent shear flow", Cambridge University Press, 1956.

(4) Rotta, J. "Statistische Theorie Nichthomogener Turbulenz, " Z. Phys. 129, pp. 547-572, 1951.

(5) Hanjalic, K. and Launder, B.E. "A Reynolds Stress Model of Turbulence and its Application to Thin Shear Flows", JFM. Vol. 52, part 4, pp. 609-638, 1972.

(6) Naudascher, E., "Flow in the wake of self-propelled bodies and related sources of turbulence", JFM, Vol. 22, Part 4, pp. 625-656, 1965.

(7) Wu, J., "Mixed Region Collapse with Internal Wave Generation in a Density-Stratified Medium", JFM, Vol. 35, Part 3, pp. 531-544, 1969.

(8) Gran, R.L. private communication

(9) Pao, Y.H., Lin, J.T., Smithmeyer, M.G. and Veenhuizen, S.D., "Internal Waves and Turbulence Generated by Submerged Bodies and Their Interaction with Surface Waves: Quarterly Report", Flow Research Note No. 16, March,1973.

(10) Schooley, A.H. and Stewart, R.W., "Experiments with a Self-Propelled Body Submerged in a Fluid with a Vertical Density Gradient", JFM, Vol. 15, Part 1, pp. 83-96, 1963.

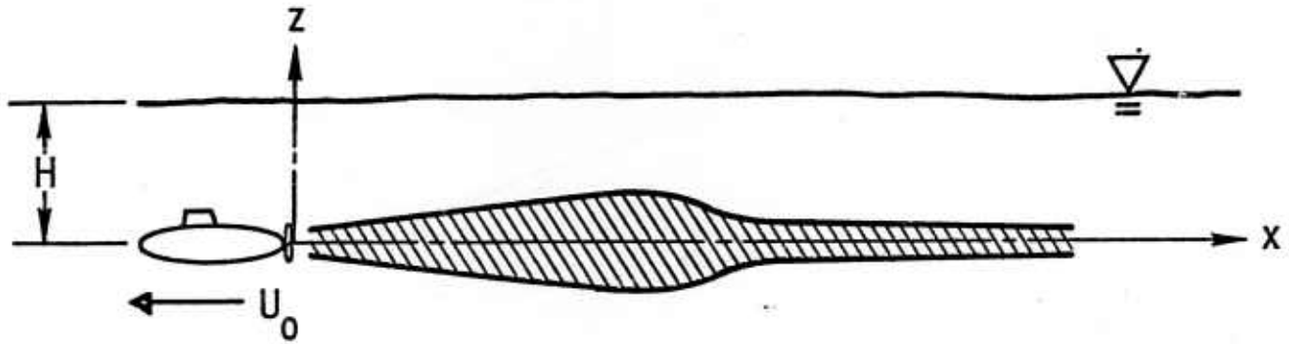

DENSITY STRATIFICATION

EXTERNAL

$\rho_0 = \overline{\rho}\ (1 - \alpha z)$

α = CONSTANT

INTERNAL

$\rho_i = \overline{\rho}\ (1 - \beta z)$

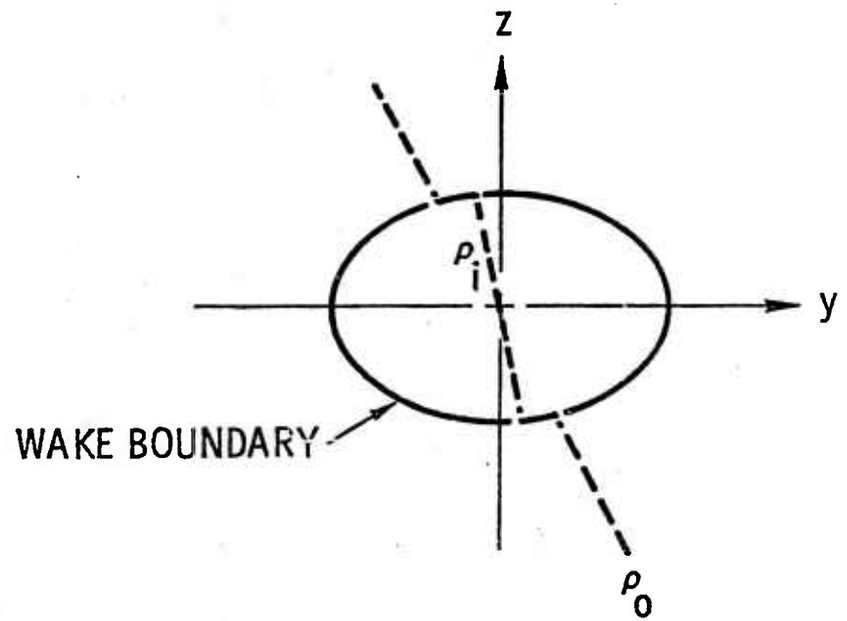

Figure 1. Coordinates and Density Field

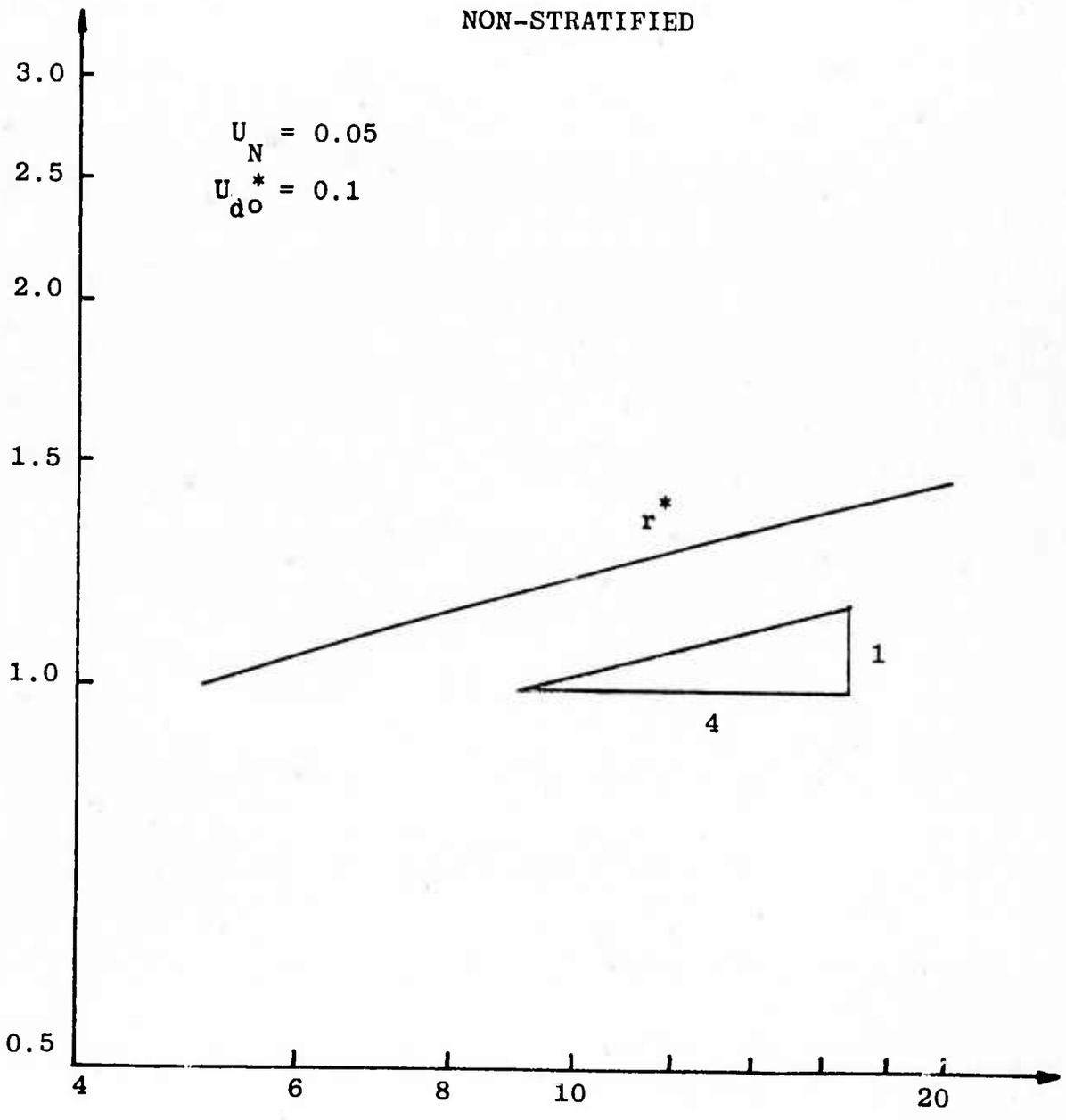

Figure 2. Calculated Wake Growth (Nonstratified)

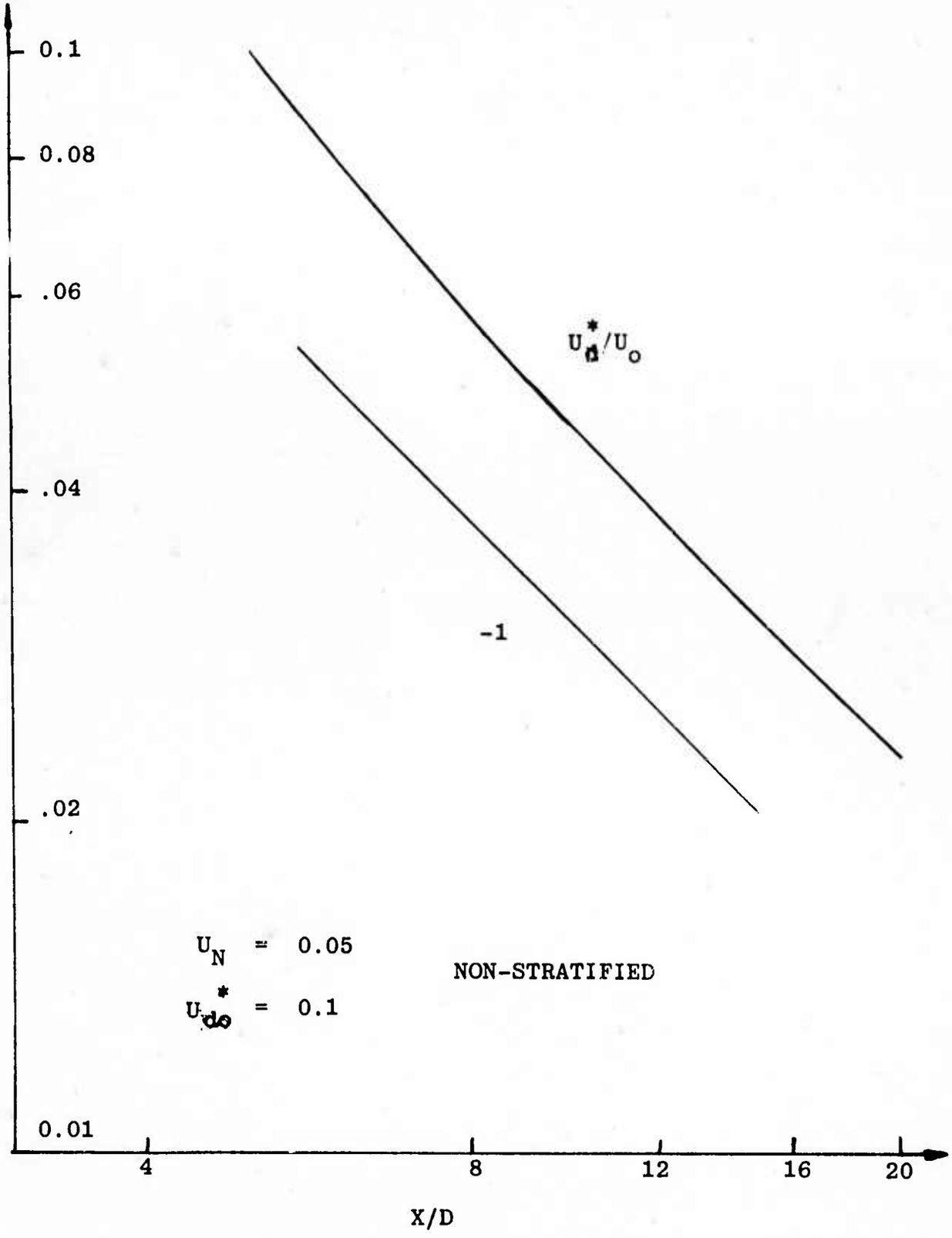

Figure 3. Decay of Mean Centerline Velocity Excess (Non-Stratified)

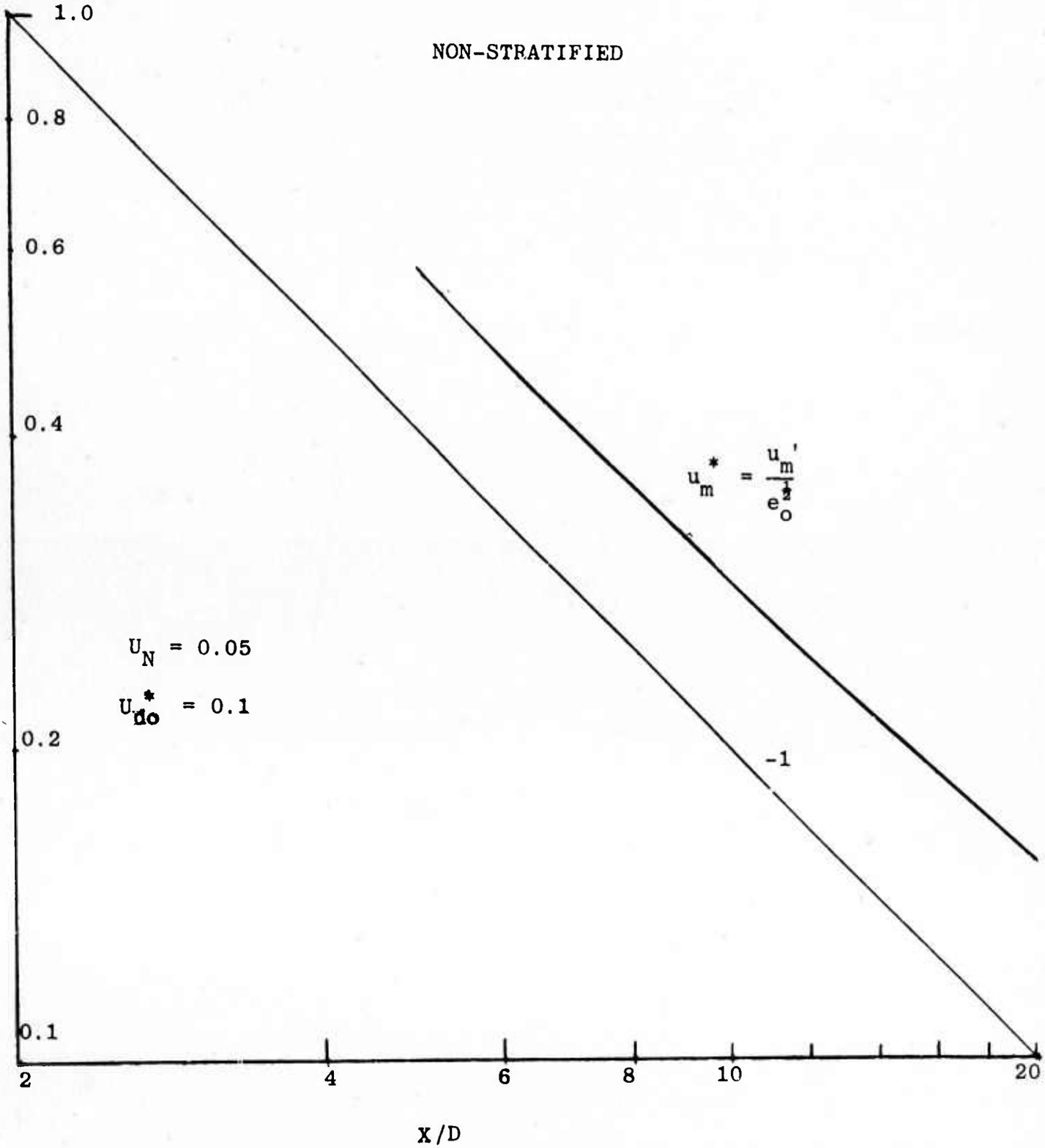

Figure 4. Decay of Turbulent Intensity (Non-Stratified).

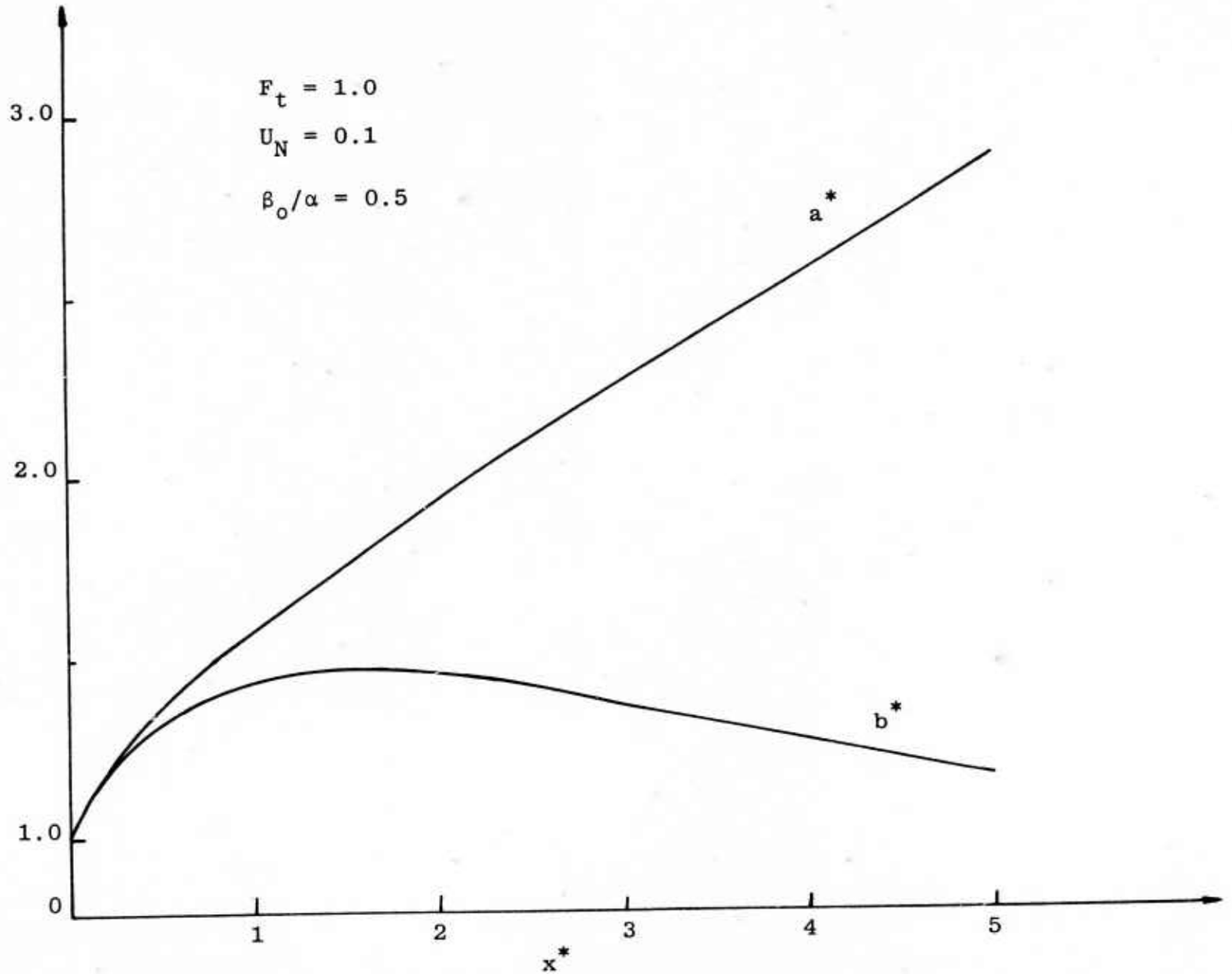

Figure 5. Typical Growth of Wake Height and Wake Width.

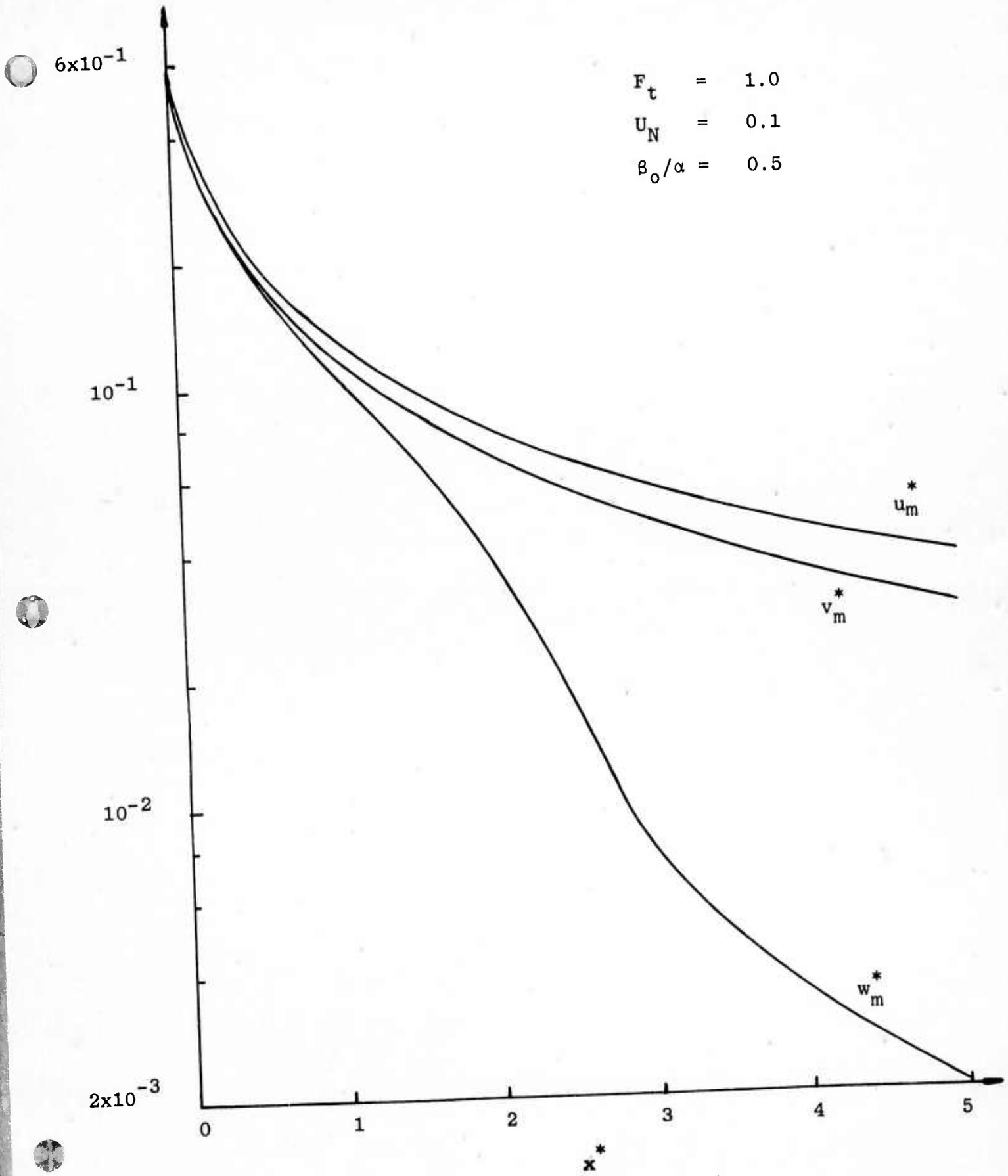

Figure 6. Typical Decay of Turbulent Components.

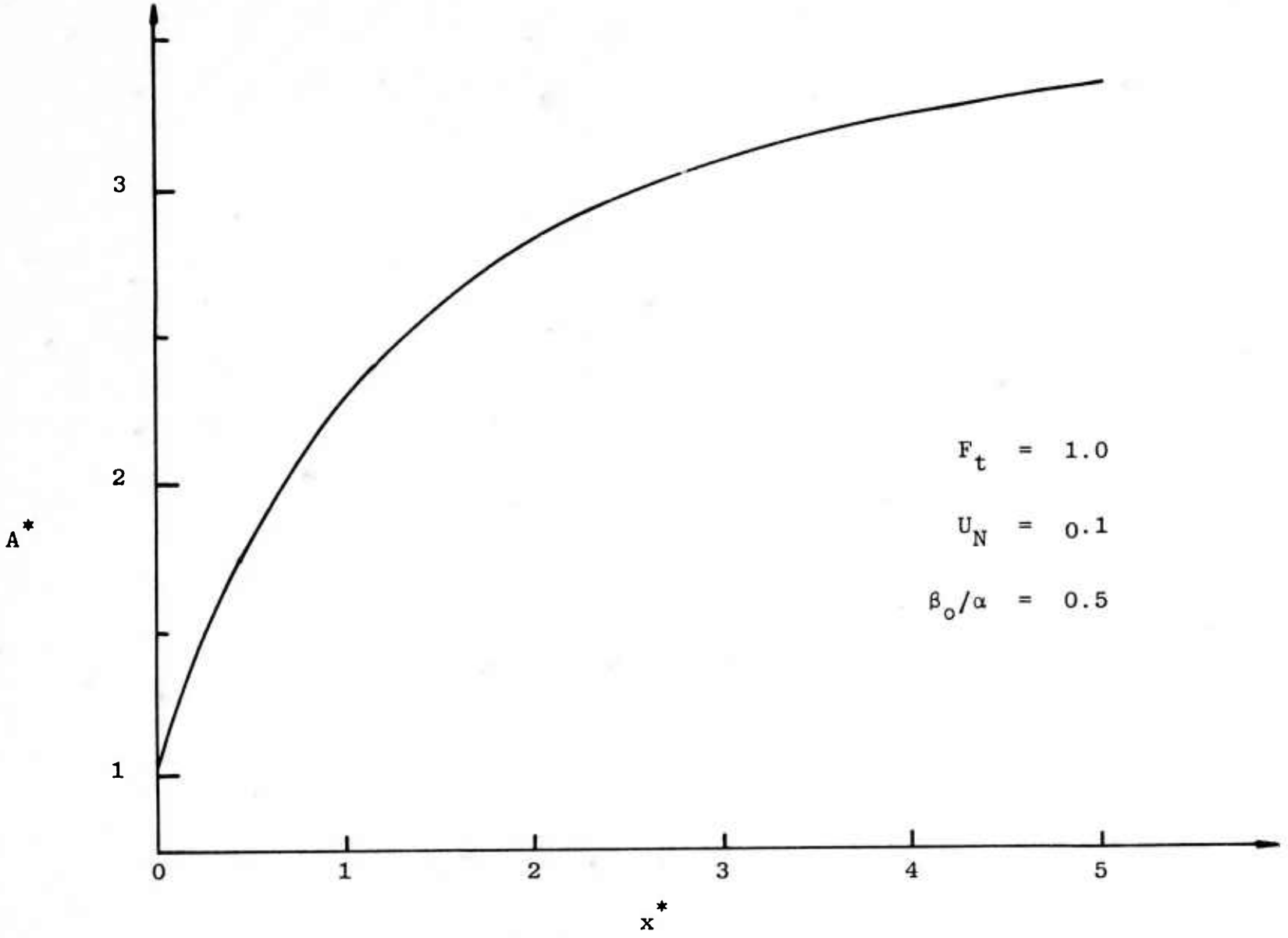

Figure 7. Typical Wake Area v.s. x^*

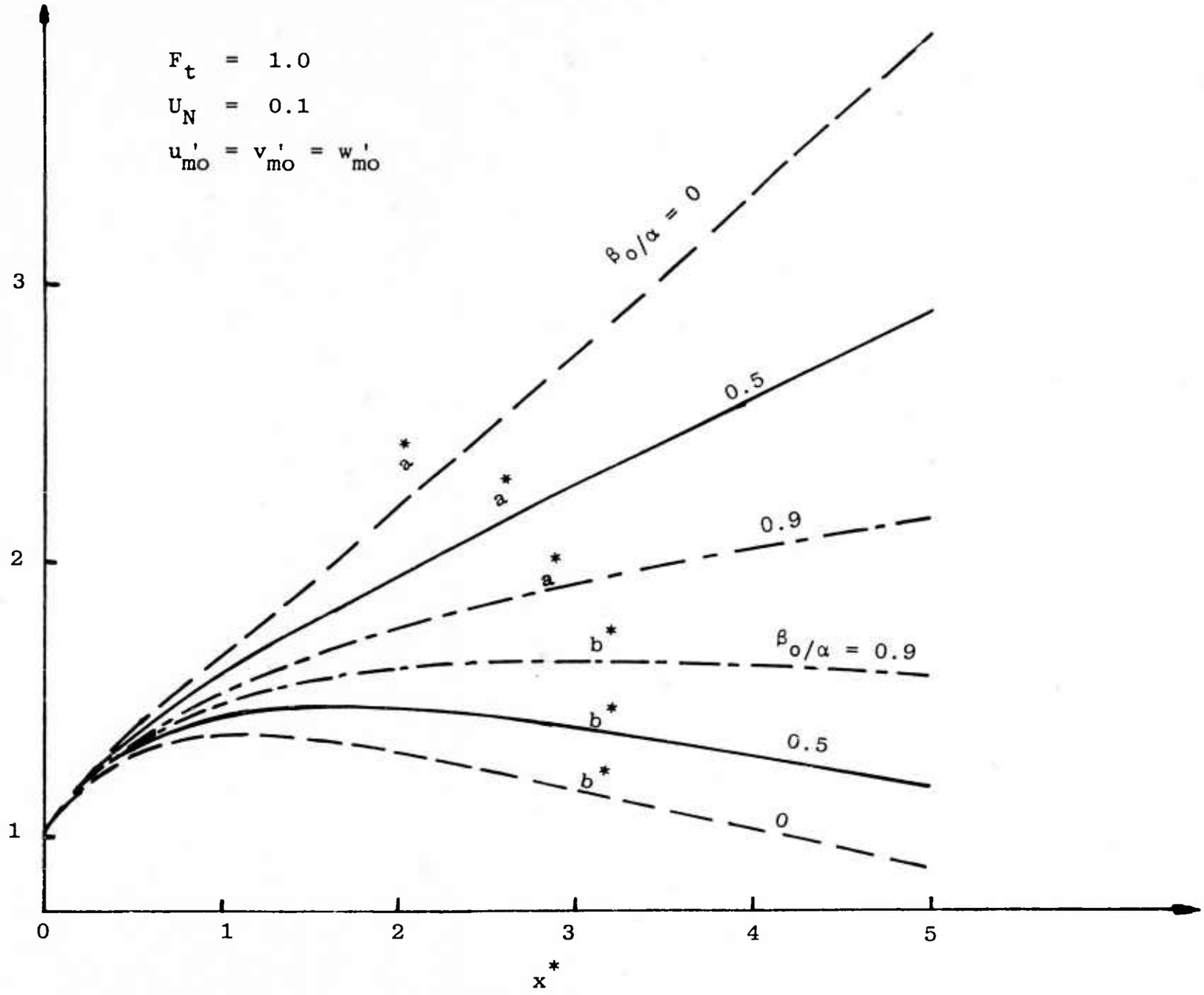

Figure 8. Effect of Initial Degree of Mixing on the Wake Geometry

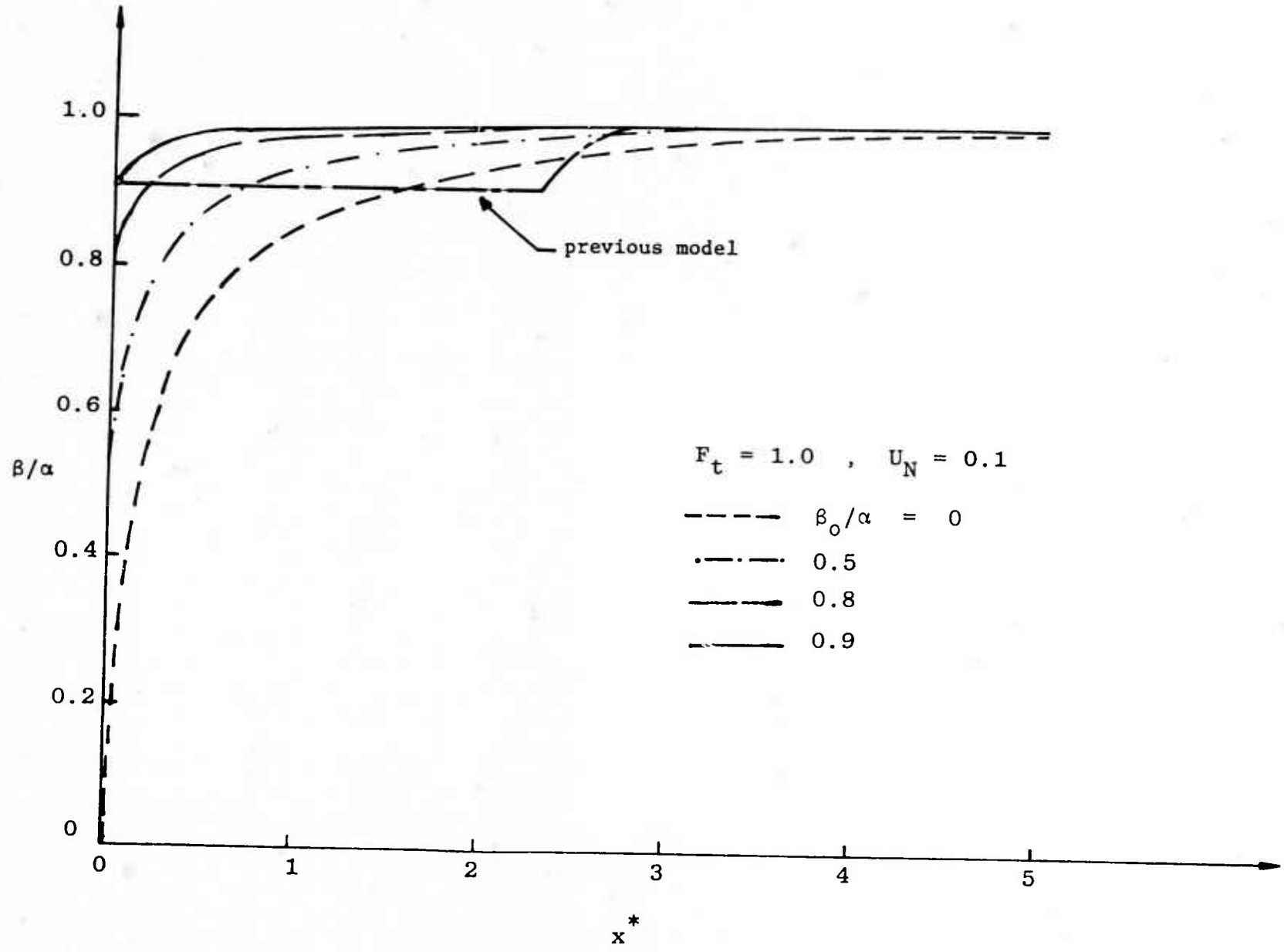

Figure 9. Variation of β/α for various β_o/α

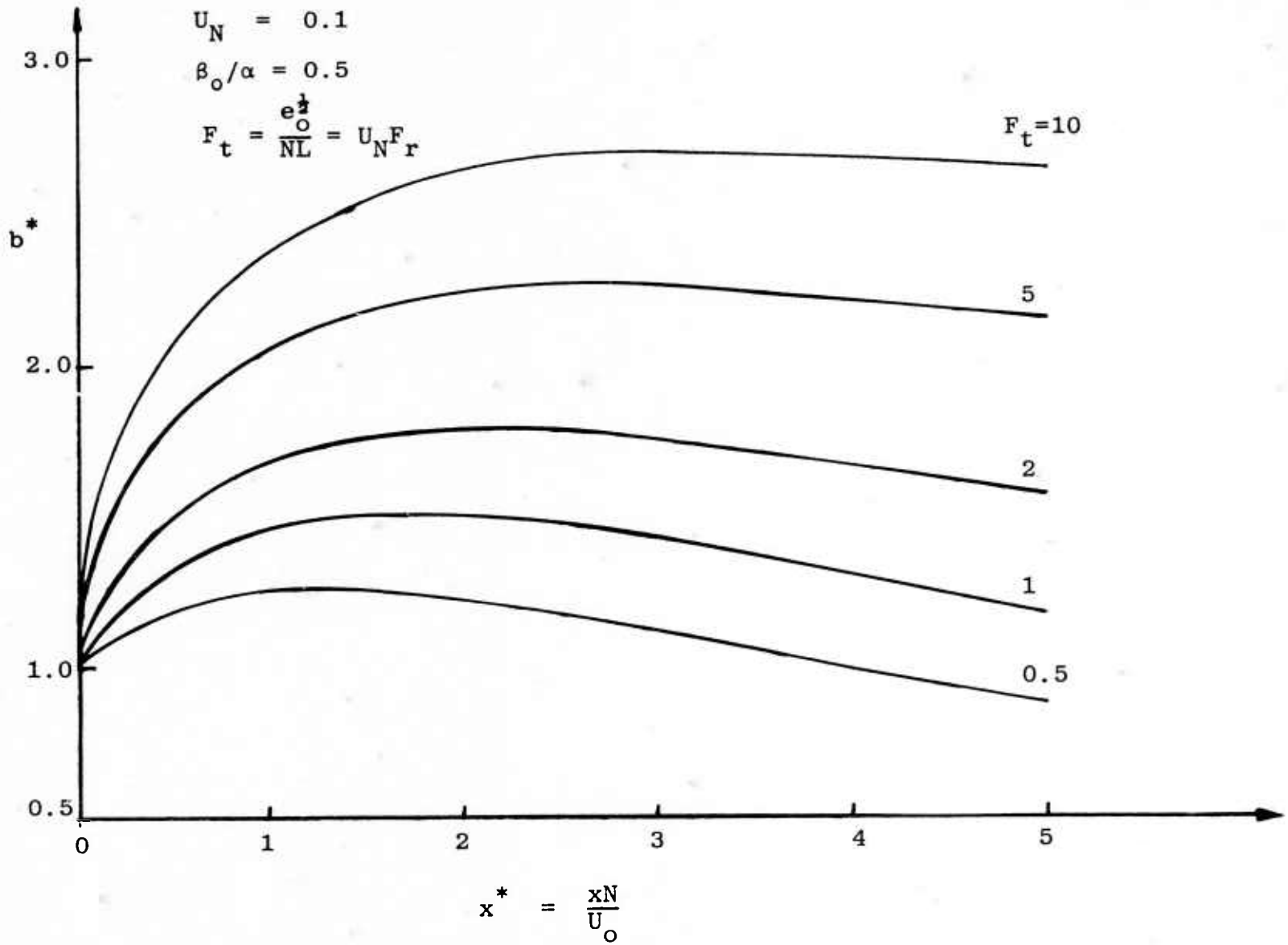

Figure 10. Dependence of b^* on the Froude Number

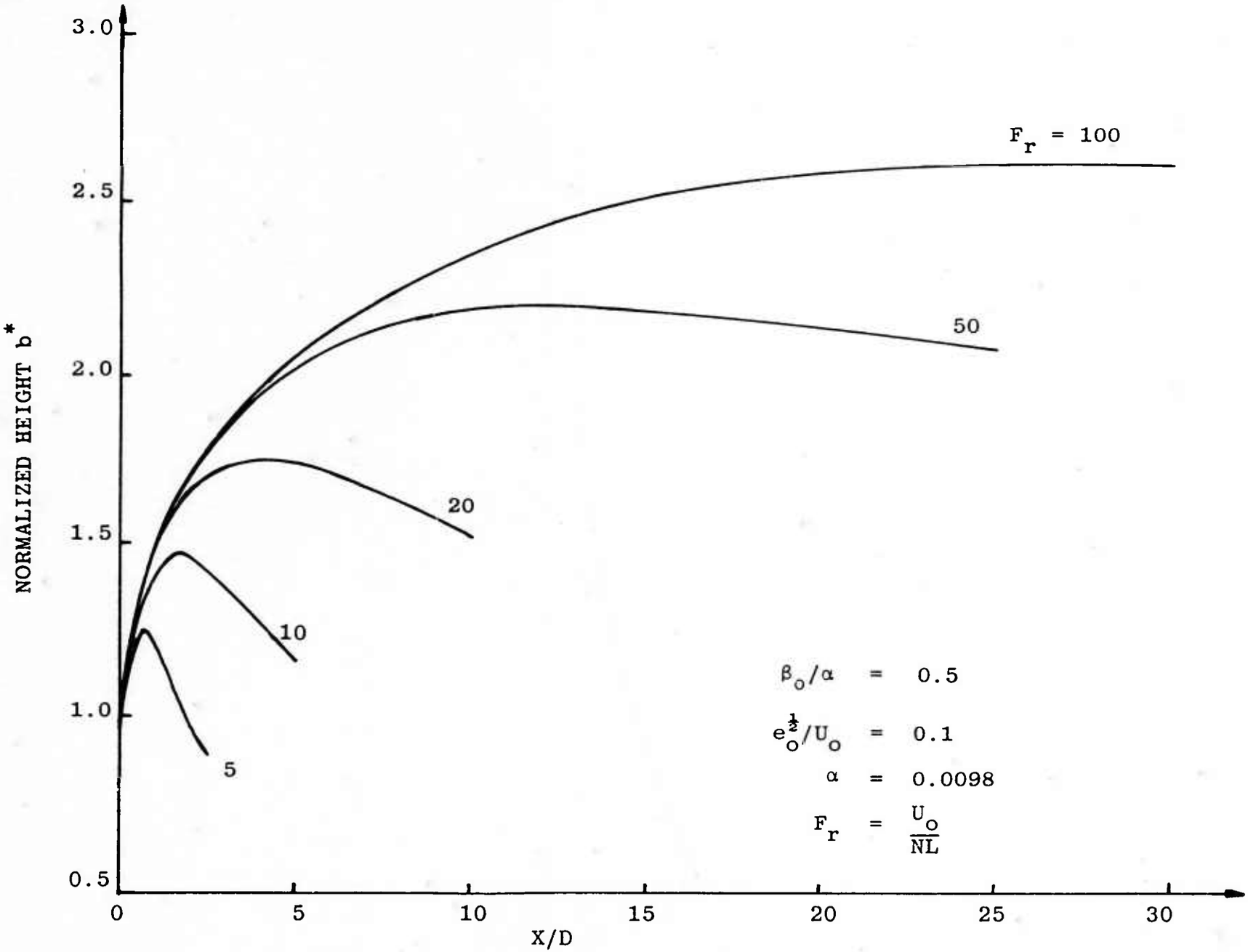

Figure 11. b^* v.s. X/D for Various F_r.

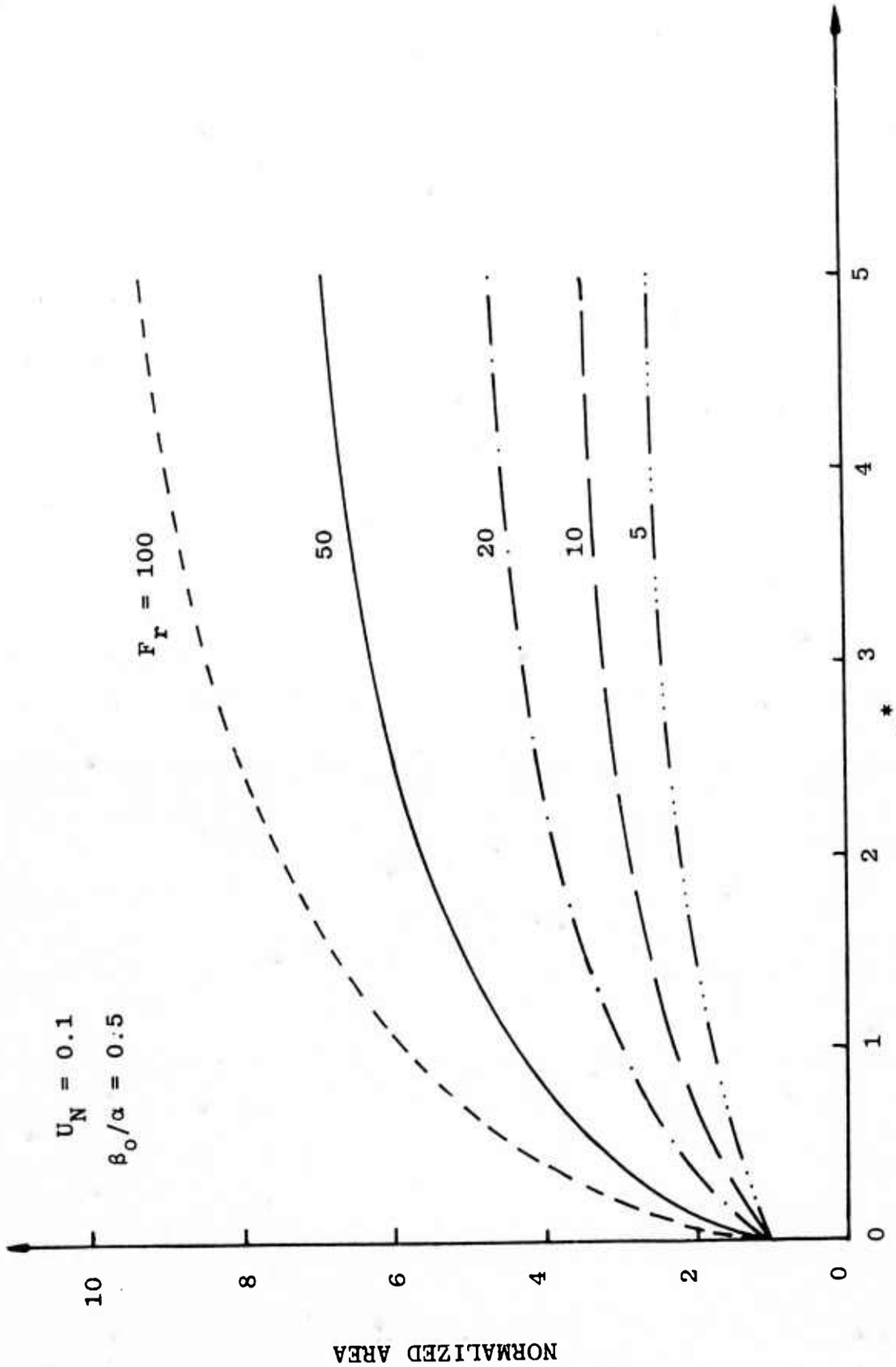

Figure 12. Effect of Froude Number on the Wake Area.

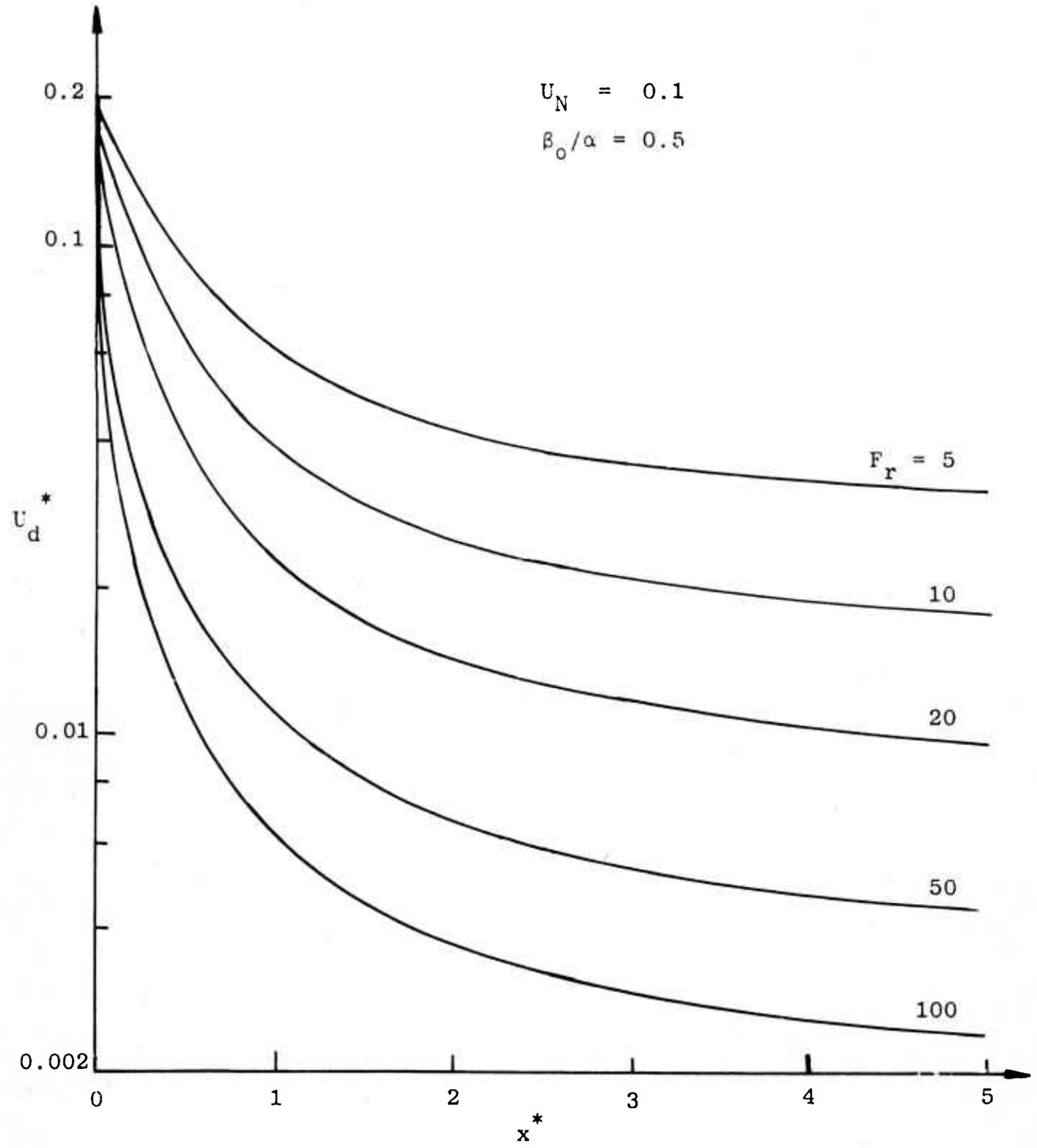

Figure 13. Effect of Froude Number on the Mean Velocity Decay.

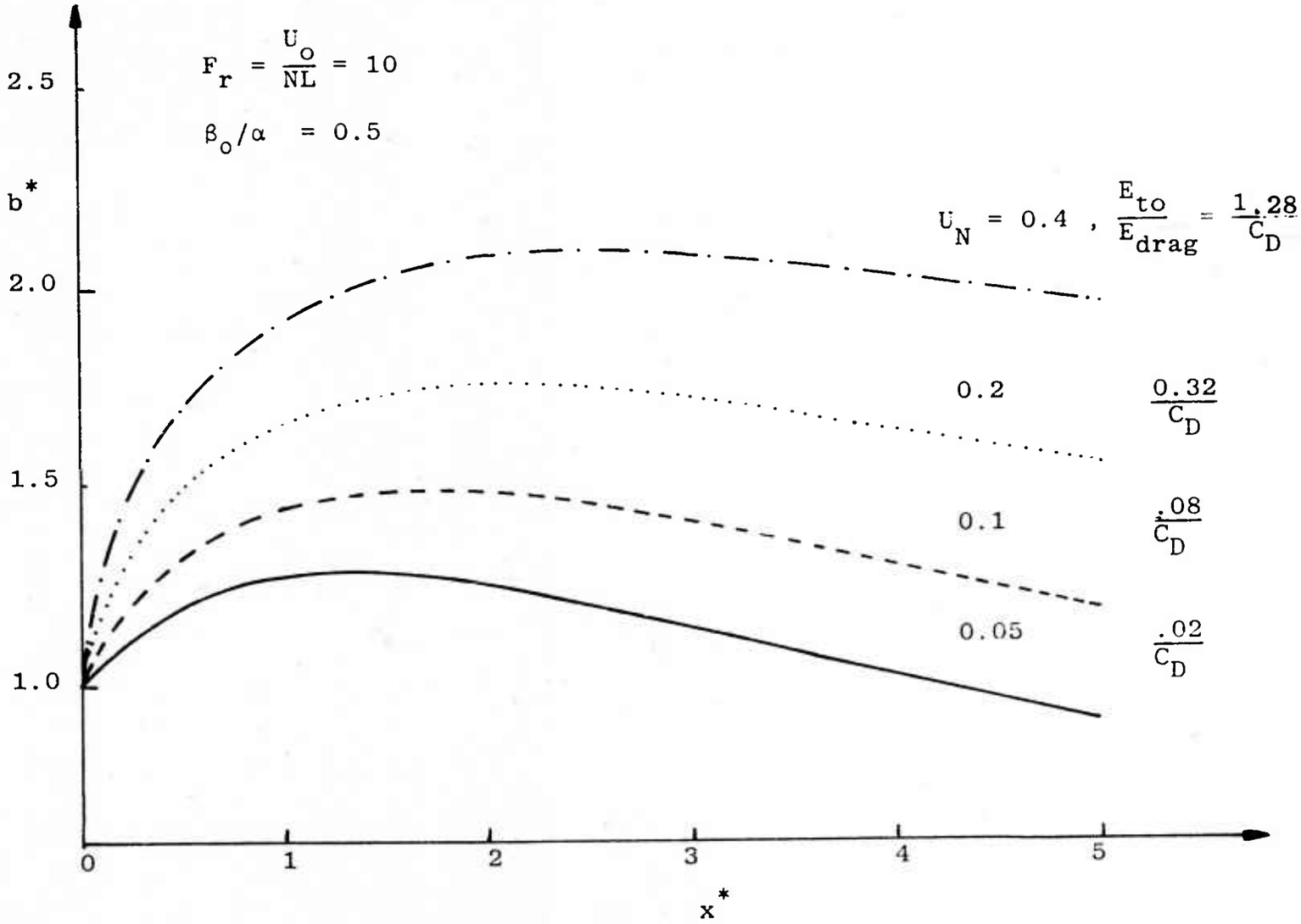

Figure 14. Effect of Initial Turbulent Intensity on b^*.

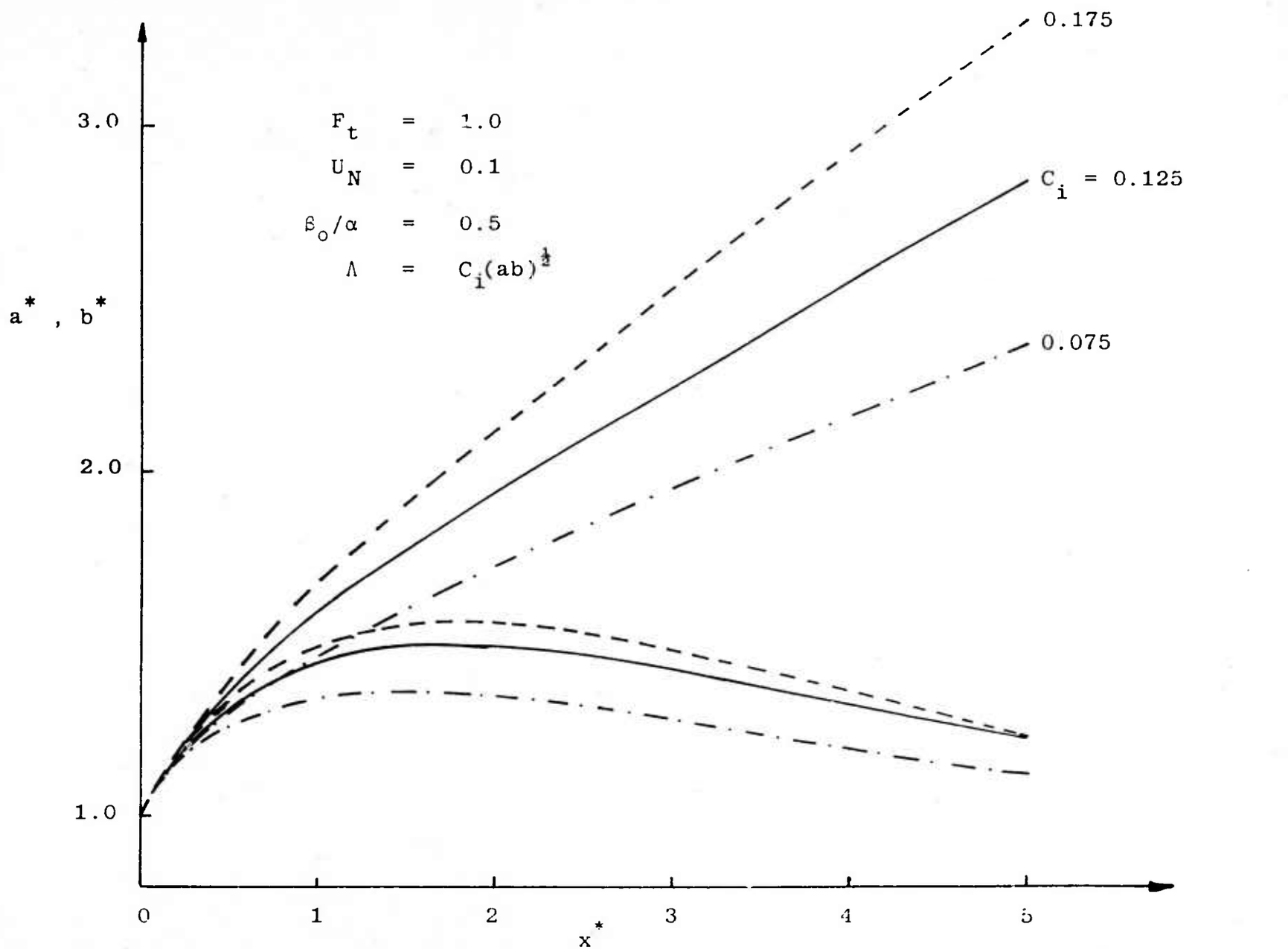

Figure 15. Effect of the Integral Length Scale on a^* and b^*.

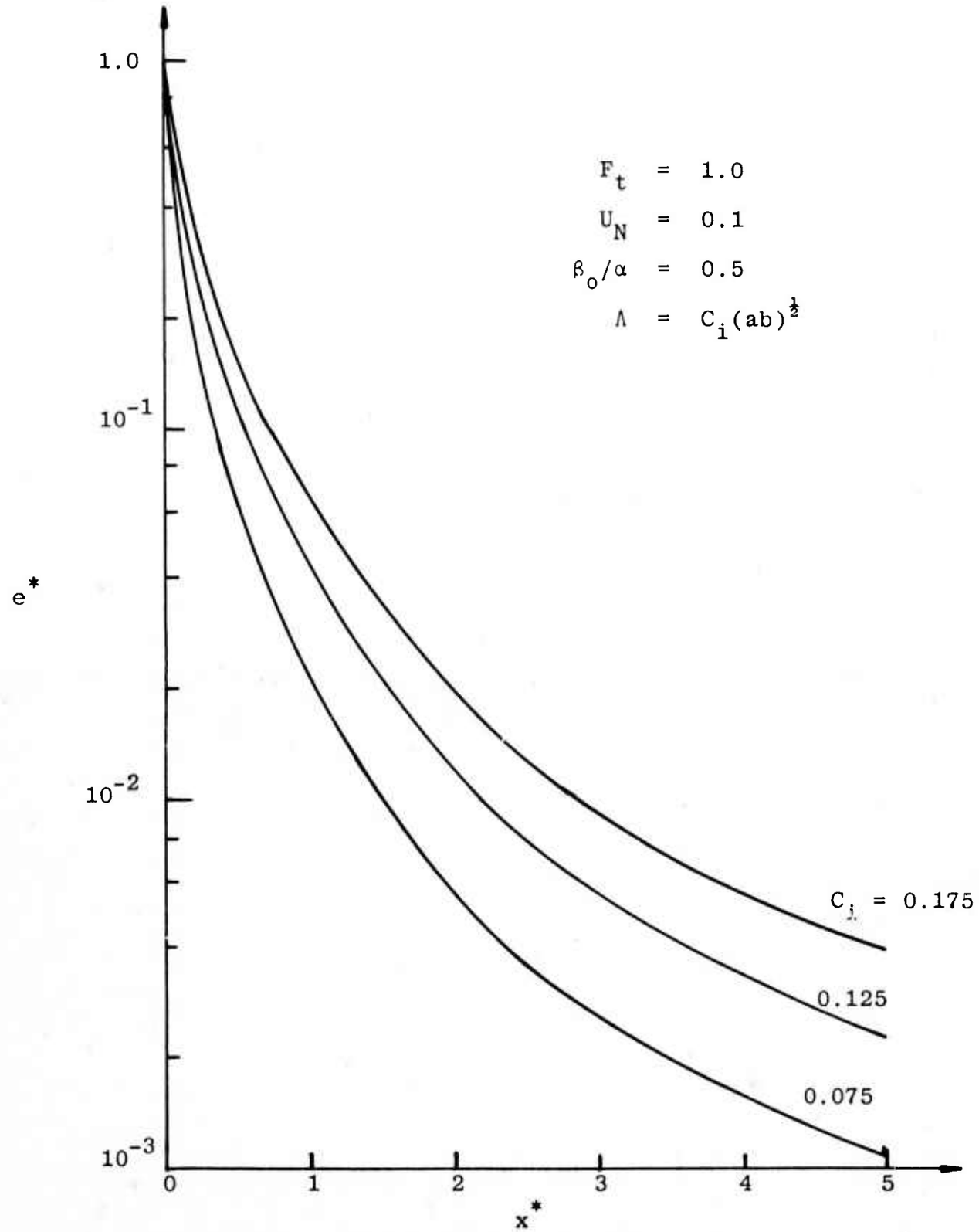

Figure 16. Effect of the Integral Length Scale on e^*

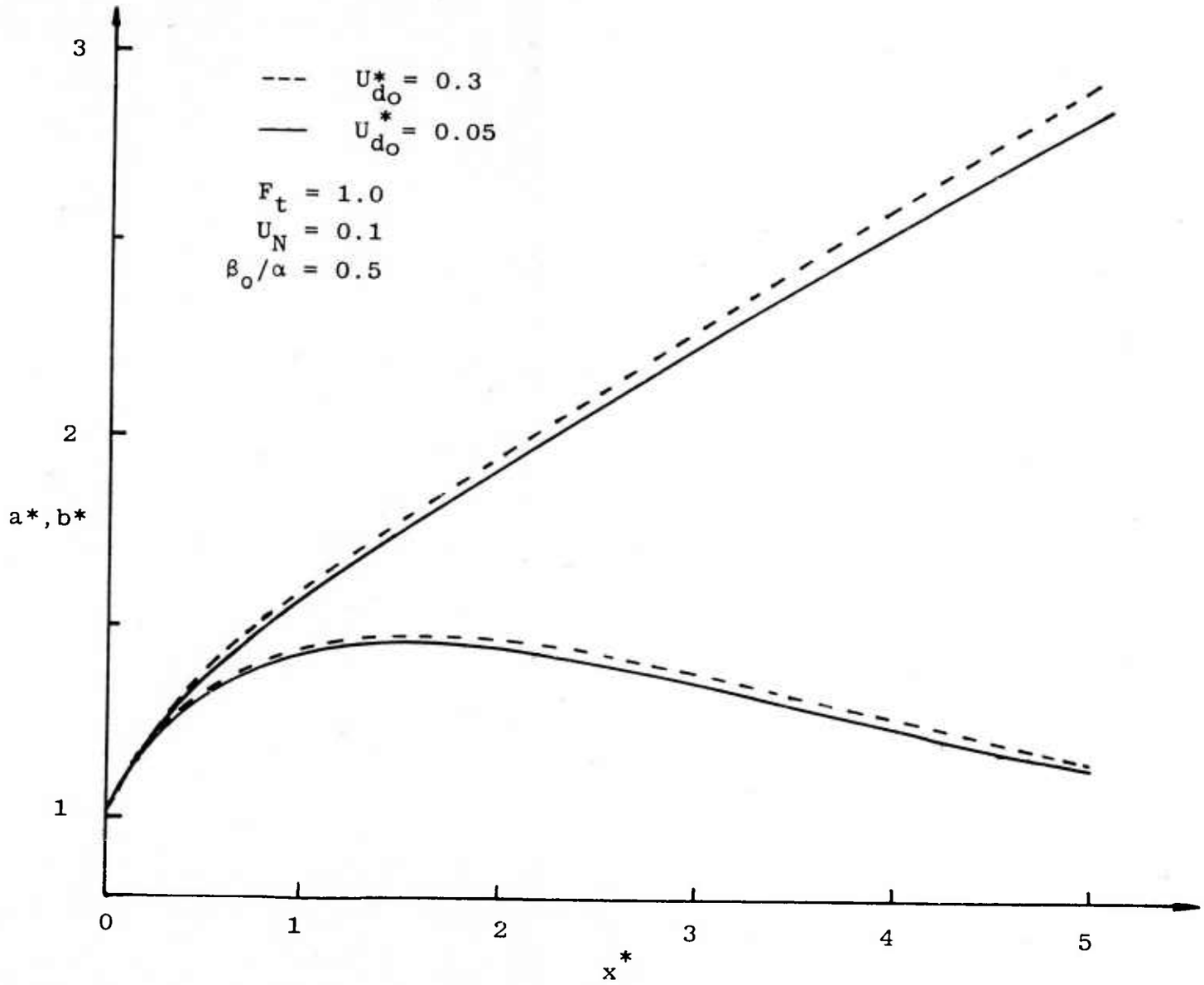

Figure 17. Effect of U^*_{do} on a^* and b^*

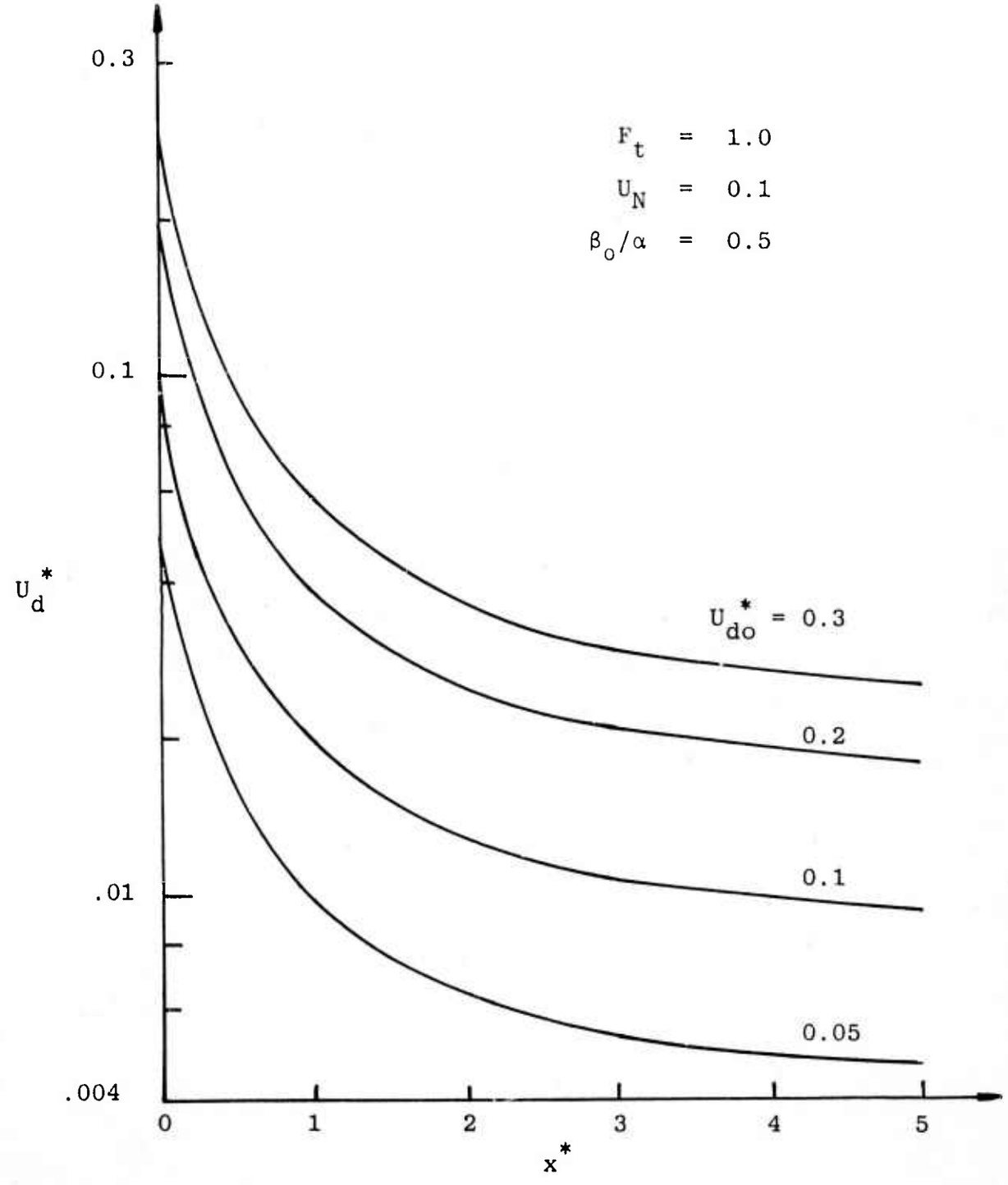

Figure 18. Effect of U_{do}^* on U_d^*

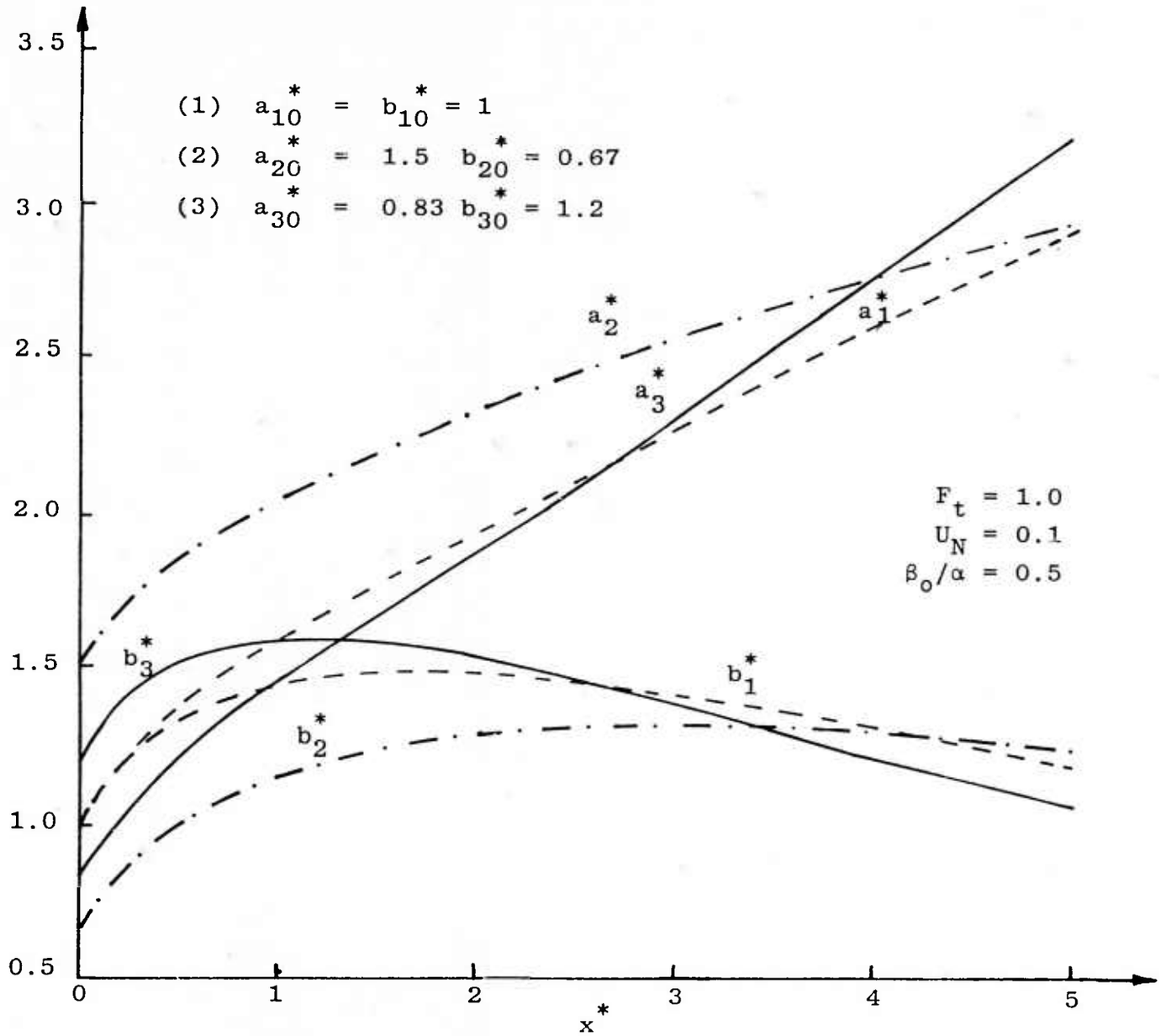

Figure 19. Effect of Initial Wake Geometry

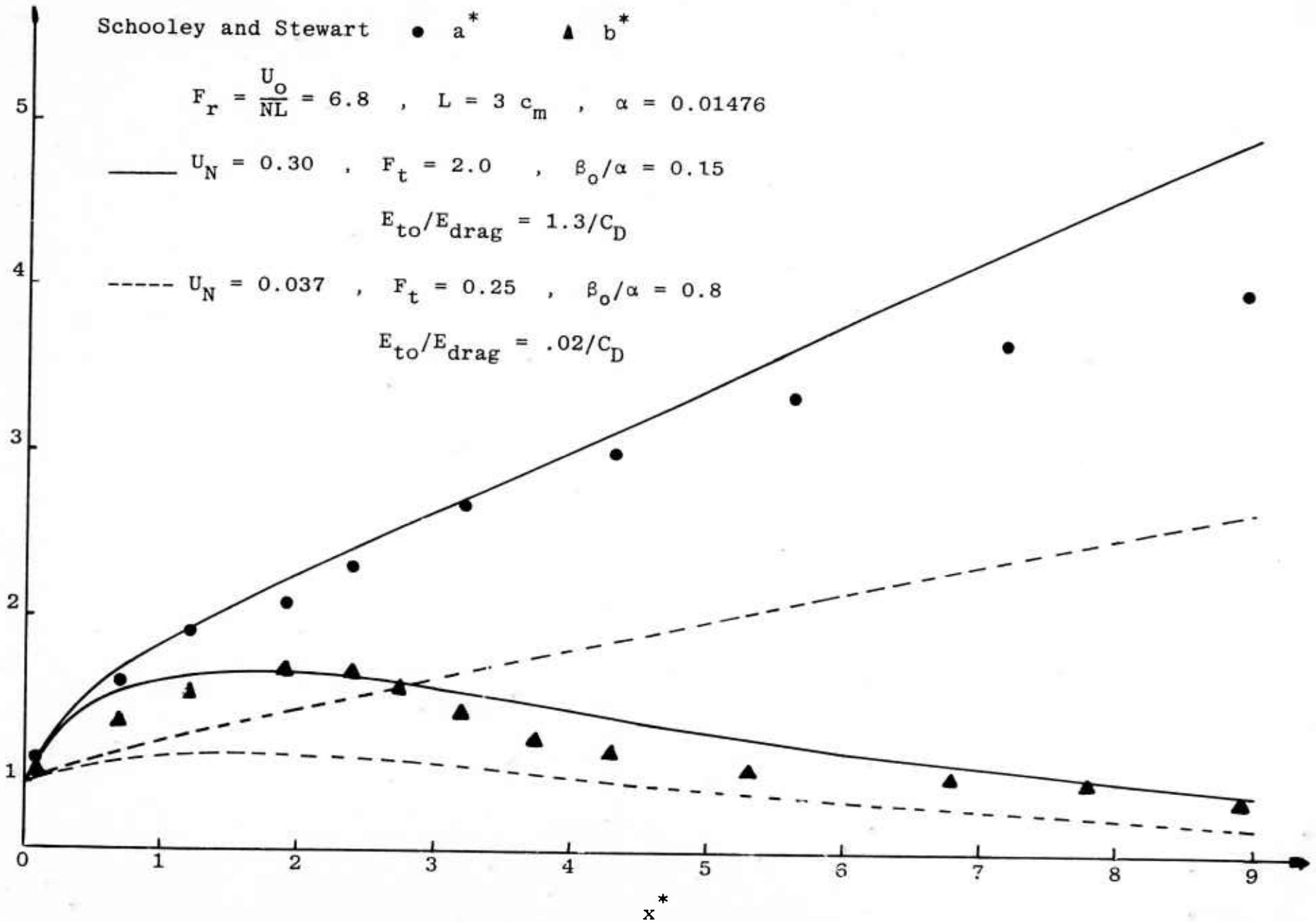

Figure 20. Comparison with the Experiment of Schooley and Stewart.